

# **Tactile Stimulation Final Report**

ECE 129: Capstone Project

**Eli Harrison-Saeli**

**Jacob Sickafoose**

June 9, 2022

# Abstract

*The market for Virtual Reality devices and experiences is growing rapidly and developers are competing to maximize their users' immersion into the virtual world. Haptic feedback is at the forefront of VR. The majority of devices use mechanical actuation to simulate virtual forces, but in doing so create cumbersome products that don't fully solve the immersion problem. Our project aims to replicate texture using transcutaneous electrical nerve stimulation. By selectively activating the nerve fibers responsible for touch, we can theoretically recreate any texture.*

# Contents

<b>1</b>	<b>Introduction</b>	<b>3</b>
<b>2</b>	<b>System-level Overview</b>	<b>4</b>
2.1	Framing Project Goals . . . . .	4
2.2	Unique Advantages of Electrical Stimulation Over Traditional Haptics . . . . .	5
2.3	Documentation of Project Goals . . . . .	8
<b>3</b>	<b>Subsystem Breakdown</b>	<b>10</b>
3.1	Electrode Array . . . . .	10
3.1.1	Theoretical Model of Nerve Stimulation . . . . .	11
3.1.2	Array Resolution Parameters . . . . .	14
3.1.3	Array Parasitic Capacitance Modelling . . . . .	16
3.1.4	Array Material Selection . . . . .	18
3.1.5	Potential New Strategies/Designs . . . . .	20
3.2	Signal Driving Circuit . . . . .	21
3.2.1	Establishing Signal Requirements . . . . .	21
3.2.2	Converting Microcontroller Signals to Meet Requirements . . . . .	23

3.2.3	Voltage and Frequency Limitations Encountered . . . . .	25
3.3	Microcontroller . . . . .	30
3.4	Glove Design . . . . .	31
<b>4</b>	<b>Mistakes Made and Subsequent Lessons Learned</b>	<b>33</b>
<b>5</b>	<b>Next Steps</b>	<b>34</b>
5.1	Our Design . . . . .	34
5.2	Nerve Stimulation in Virtual Reality . . . . .	34
<b>6</b>	<b>Appendix</b>	<b>35</b>

# 1 Introduction

Current Virtual Reality systems don't provide realistic tactile feedback. The majority of emergent haptic feedback technologies target force feedback, neglecting the tactile dimension. This means they are using resistance against movement to simulate virtual objects while entirely ignoring their textures and finer details. Simulating tactile sensation would be a huge improvement for user immersion in Virtual Reality. Our project aims to deliver a peripheral nerve interface integrated into a wearable glove that can provide a realistic simulation of texture using transcutaneous electrical nerve stimulation.

Virtual reality has seen massive mainstream attention in recent years. Novel VR technology is constantly being applied in a variety of different fields, from entertainment to medicine. This was massively accelerated due to the unforeseen COVID-19 pandemic which limited physical social interactions. In 2020 the global market for haptics hit an estimated US\$13.8 Billion amidst the pandemic. The market for haptics simulation is projected to hit \$28.1 Billion by 2026.

Our solution achieves a greater degree of realism than traditional mechanical haptic feedback by bypassing the mechanoreceptors in the skin and interfacing directly with the nervous system. This allows for a far more dynamic range of stimuli that would not be achievable with mechanical actuators. Transcutaneous electrical nerve stimulation allows for great control over the nervous system without the invasiveness of an implanted computer-nerve interface.

Our project takes the form of a haptic feedback glove. A microcontroller mounted on the glove interfaces with the user's computer that is running a VR simulation. Based on the needs of the simulation, the microcontroller drives electrode arrays which line the inside of the glove. The electrodes inject current through the skin in order to illicit a specific nervous response. The stimulation patterns are designed to induce the perception

of texture in the user; the texture corresponds to the surface of the virtual object the user is making contact with in the VR simulation.

## 2 System-level Overview

### 2.1 Framing Project Goals

As we move into describing the goal for the project that we originally defined, we first need to address the glaring disconnect between the haptic solution that we theorized and the more realistic goal that we actually worked towards and nearly completed.

The system we believed could succeed in the market is defined in our project proposal which we developed in the Fall as well as in the supporting documents including the Success Criteria Matrix, Concept of Operations Flowchart, and Repository for System Requirements. This device was envisioned to compete by meeting the market demand for a sleek, highly realistic, and user friendly haptic feedback system focused on creating an authentic simulation of texture. This device would be capable of replicating virtually any texture and be optimized for an ergonomic and frustration-free user experience. While bringing such a device into reality is still the overarching motivation for our project, we ultimately lacked the means to develop such a system.

Given our limitations, the true goal for this development stage of the product is a simple proof of concept that validates the fundamental operation of an electrically actuated haptic feedback system. We shifted our focus to creating a minimum viable product, the primary goal being to produce a distinguishable stimulus using only transcutaneous electrical stimulation. By sacrificing all the nonessential features we initially envisioned, we were nearly able to achieve this proof of concept. Unfortunately, we ultimately did not satisfy our main goal of producing stimulus. The specific goal as well as what we *did* accomplish will be further detailed.

## 2.2 Unique Advantages of Electrical Stimulation Over Traditional Haptics

We were willing to undertake this difficult project because we firmly believe that electrical stimulation based haptics are positioned to fill the aforementioned market demand for high quality VR sensory simulation. In Figure 1, we use SWOT analysis to highlight some of unique advantages that electrical stimulated haptics have over the traditional mechanically actuated haptic that dominate the emerging market and R&D space today.

Ultimately, perfect VR immersion will be enabled by brain-computer interfaces (BCI) that will be able to directly actuate any nerve in the body and brain, eclipsing all other forms of haptic feedback and removing the need for any stimulus external to the user. However, BCI technology is vastly more technically challenging than our transcutaneous system, and is likely decades away from commercial viability. VR developers are in an arms race to fill the market during this vacuum. Figure 2 depicts our interpretation of where different haptic feedback technologies fall on the spectrum of invasiveness versus the level of control over the nervous system which translates to quality of VR immersion.

Vibrational haptic feedback, plotted on Figure 2, is something most people are familiar with. A simple vibration that adds tactile feedback to any number of devices. The most common example of this is the vibration of modern smart phones experienced when the home or back button is pressed. Vibrations are also utilized in VR controllers and very simple haptic feedback gloves. One step above vibrational feedback is mechanical force feedback. This uses mechanical actuators to produce a reaction force against the body in order to simulate the resistance of a virtual object. This technology has so far been limited to products still in development such as HaptX's DK2. These two mechanical approaches are fundamentally limited in their control over the nervous system, as

# SWOT Analysis of Electrical Stimulation Haptic Feedback System

Strengths	Weaknesses	Opportunities	Threats
<ul style="list-style-type: none"> <li>• Unique ability to simulate texture</li> <li>• Scalability from simple design</li> <li>• Ergonomic and lightweight design</li> </ul>	<ul style="list-style-type: none"> <li>• Cutting edge technology means lack of background research</li> <li>• Very technically demanding to develop</li> </ul>	<ul style="list-style-type: none"> <li>• Rapidly growing market for haptic feedback devices</li> <li>• Lack of competition in texture simulation</li> </ul>	<ul style="list-style-type: none"> <li>• Competitors developing mechanical haptic devices with large budgets and years of development</li> <li>• Made obsolete by brain-computer interfaces</li> </ul>

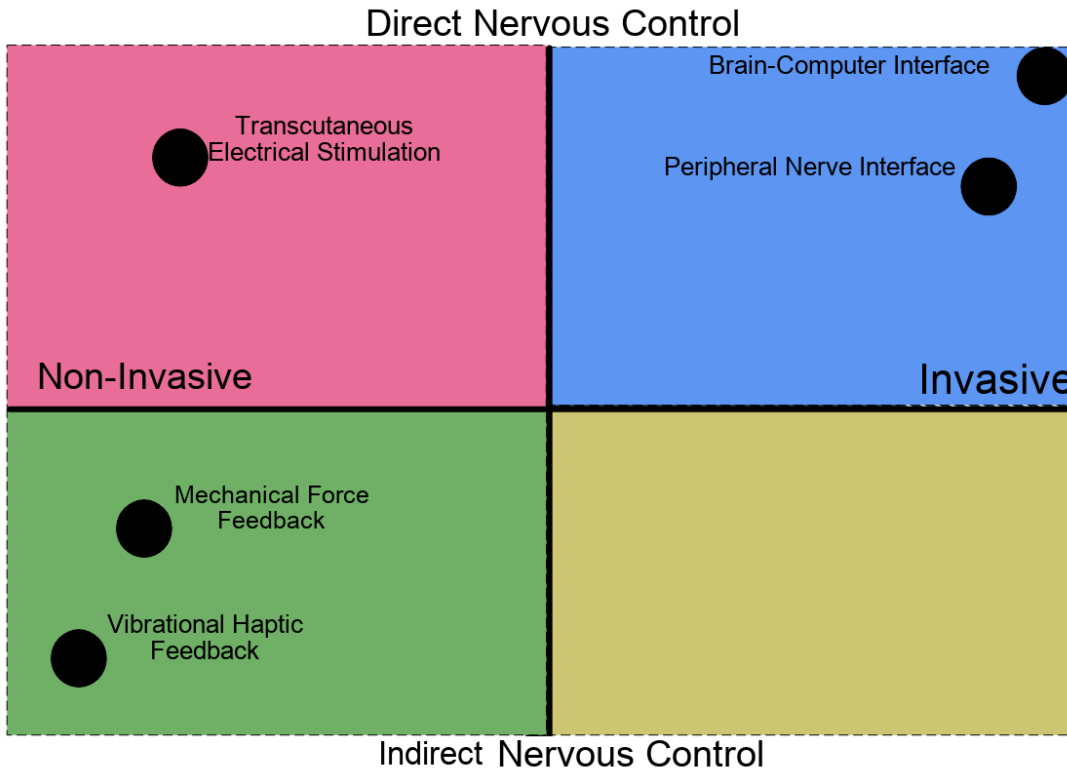
V1 6/9/2022

Figure 1: SWOT analysis of electrical haptic systems helps us identify the unique position of this technology in the field of haptic. Despite difficult technical challenges and fierce competition for large companies such as Meta and HaptX, electrical stimulation technology has fundamental advantages that make it a project worth pursuing.

they actuate nerves indirectly through mechanoreceptors in the skin and muscles in the hand and arm. Their ability to induce a sensory response is limited by the receptors they can stimulate, resulting in their low score on the nervous control axis. Their main advantages are that they are less invasive than direct nerve interfaces and they use technology from the well established field of mechanics.

A brain-computer interface is an electrical system directly integrated into the brain, potentially capable of recording and inducing the nervous activity responsible for any form

# Nerve Interface Control-Invasiveness Tradeoff



V1 6/9/2022

Figure 2: The tradeoff between invasiveness and control over the nervous system shows a comparison between different haptic technologies. Mechanical systems are non-invasive but suffer from limited control over the nervous system. Future implanted nerve interfaces will have unparalleled control over the nervous system, but will require invasive surgery to install. Our transcutaneous electrical system benefits from aspects of both alternatives. Each point is described in depth in Section 2.2.

of perception. Peripheral nerve interfaces are less invasive, as they are integrated outside of the brain (in the peripheral nervous system) and could provide control over any body part downstream of the interface. We consider both as highly invasive as they require some form of surgery to install.

Our approach, transcutaneous electrical nerve stimulation, is uniquely positioned in that it is far less invasive than other nerve interfaces yet still bypasses the mechanore-

ceptors to interface directly with the nervous system.

### 2.3 Documentation of Project Goals

The project goals for a final product are documented between our Repository for System Technical Requirements: Figure 28, our Concept of Operations Flowchart: Figure 29, and Success Criteria Matrix: 30. These are all included in the Appendix for reference.

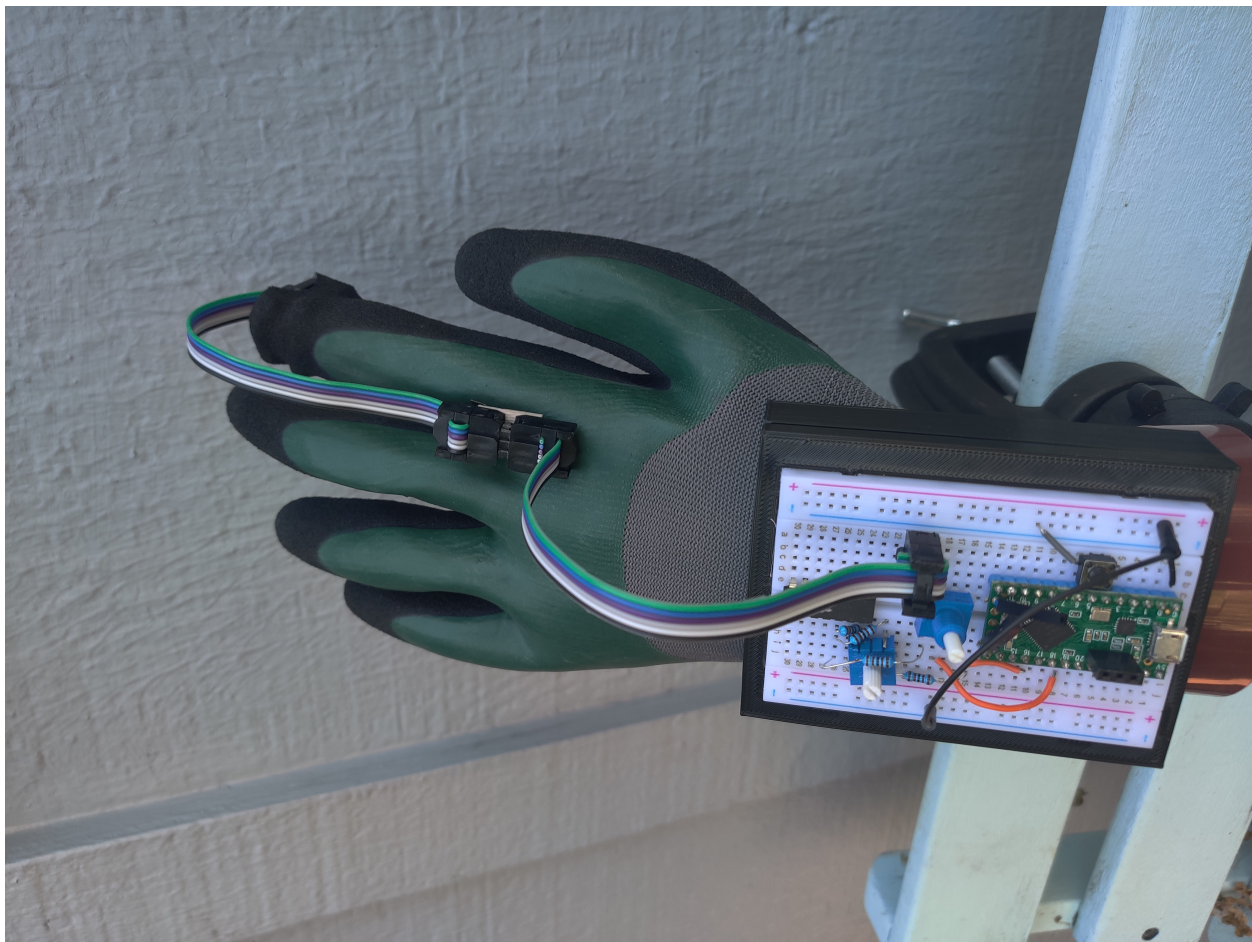


Figure 3: Image of final proof of concept prototype glove.

Our proof of concept system is pictured in Figure 3 and its basic functionality is represented by our System Block Diagram in Figure 4. A full wiring diagram including theoretical models of the load is depicted in Figure 5.

## Dove System Block Diagram

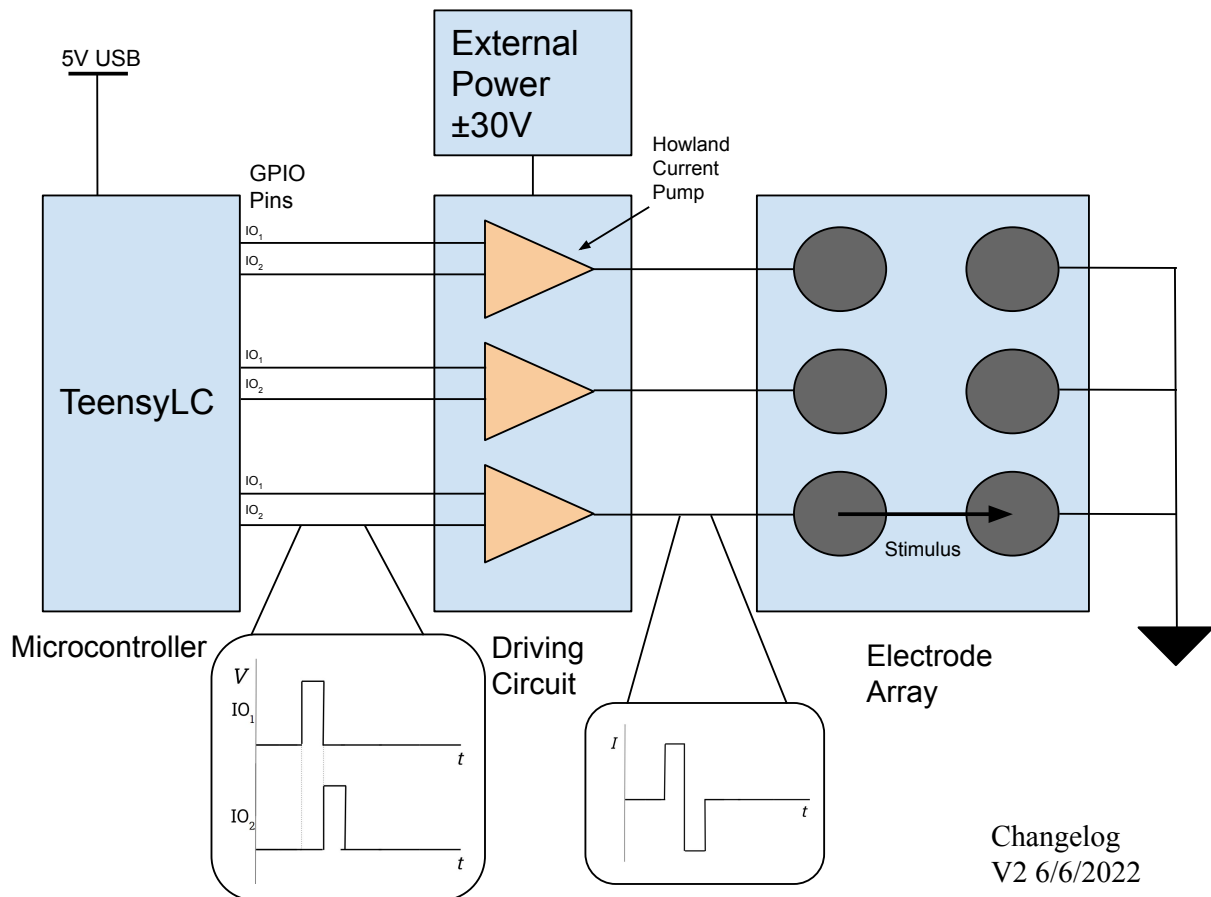


Figure 4: This is a system block diagram of what our proof of concept looks like. The TeensyLC microcontroller provides a waveform to the driving circuit. The circuit, powered by a 30V desktop power supply, drives a current wave through the electrode array, applying the stimulus to the user's skin.

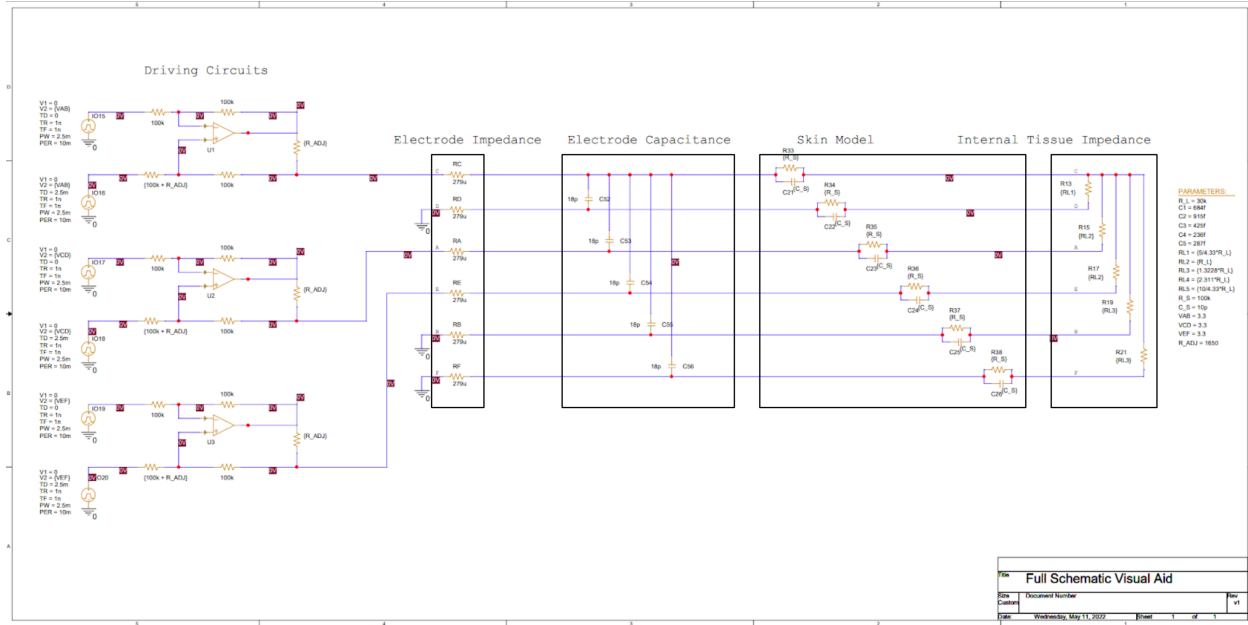


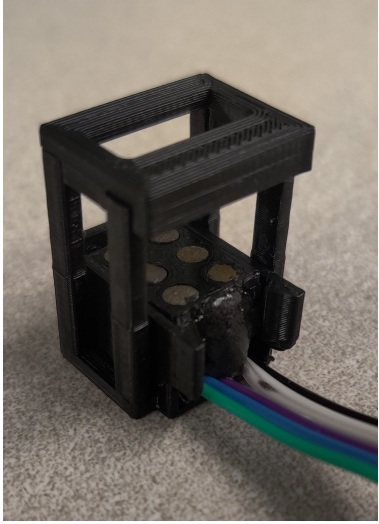
Figure 5: This is a wiring diagram of our system. It shows the Howland current pumps (in reality we built only 1, not 3), their connections to the IO pins of the microcontroller, and our best theoretical models of the load impedance divided across the electrode resistance and capacitance, the skin, and the internal tissue.

### 3 Subsystem Breakdown

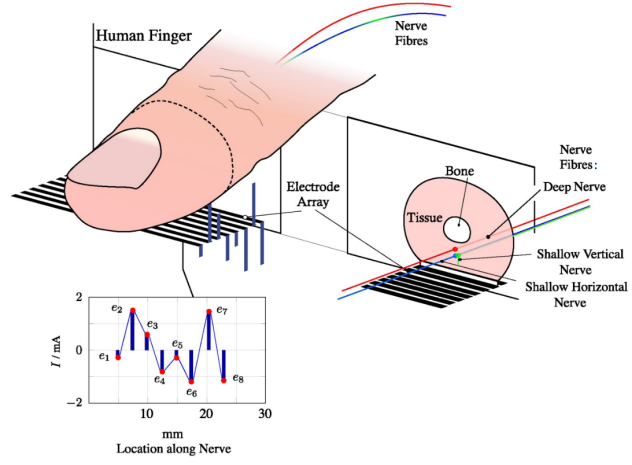
Our proof of concept prototype is comprised of four subsystems: the electrode array, driving circuit, microcontroller, and mounting hardware. All subsystems are complete enough to function as a minimum viable product with the exception of the driving circuit. The functionality and status of each subsystem is discussed in detail in the following sections.

#### 3.1 Electrode Array

The first of the subsystems to be covered is the electrode array. Our proof of concept prototype features a six-electrode array which cradles the fingertip inside the glove. The array is sized to not inhibit flexion of the finger.



(a) Image of proof of concept electrode array in finger mount.



(b) Visual aid depicting surface electrodes in relation to target sensory nerves [1].

Figure 6: The electrode array subsystem prototype and theoretical application.

By running current through the fingertip via these electrodes, an electrical potential gradient is created inside the body and along the length of the nerve cells. Once this gradient causes the potential drop across the membrane of the nerve cell to reduce to a certain threshold, an action potential is generated which travels through the nervous system to the brain. By modulating the potential gradient via changes in the stimulus patterns, we can selectively activate nerves based on their depth and orientation. With the selective activation of the four types of nerve responsible for tactile sensation, we have the ability to simulate a wide range of textures.

### 3.1.1 Theoretical Model of Nerve Stimulation

In order to inform the design of all our subsystems, we need to understand the theoretical mechanisms by which an electrical stimulus can create the sensation of texture. The mechanism for the activation of individual nerve fibers is explained in Figures 7 and 8.

Selective activation was demonstrated to be possible by Illan et. al. though a finite ele-

ment model of the electrical characteristics of the skin and touch responsible nerves [1]. Their findings are depicted in Figure 9. From an 8-electrode array, for a given waveform, one nerve type is able to be activated without the activation of another type in the same area. Since this publication, other researchers have recreated this effect *in vivo*. There are 4 mechanoreceptors responsible for effectively all sensations of touch, and each one connects to a different type of nerve: the RA, PC, SA1 and SA2 nerves, depicted in Figure 7(a). Selectively activating these four nerves enables the recreation of the same nervous response that would naturally occur when touching any given texture.

There also arises the need for the current wave to be biphasic and symmetrical in order to balance the amount of charge going in and out of each electrode. An imbalance could result in the uneven concentration of ions at the interface of the electrode which would inhibit further charge from passing through the interface. Additionally, the electrical charge can catalyze redox reaction in the electrode. If the charge is balanced quickly, the majority of these reactions will be reversed. If not, the imbalance could cause corrosion on and in the electrode. Waveforms conforming to this constraint are depicted in Figure 10. We are using the symmetric biphasic pulse.

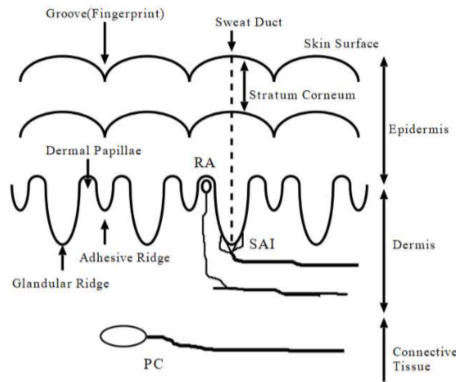
Research on the impedance of the skin and skin-electrode interface shows that the resistance is heavily dependent on environmental factors. This variable bio-impedance can be the result of variations in the thickness and number of inhomogeneities in the skin, amount of subcutaneous fat, humidity and moisture (especially a concern if the glove causes the hands to sweat), and pressure of the electrode against the skin. Because of this, the ideal driving circuit is a constant current source rather than constant voltage source to ensure the applied current does not vary based on impedance changes. It is ultimately the current that creates a small voltage drop across the internal tissue, whose impedance does not vary as much as the epithelial tissue. This is what creates the potential drop in the tissue that depolarizes the membrane potential of the target nerve,

resulting in an action potential.

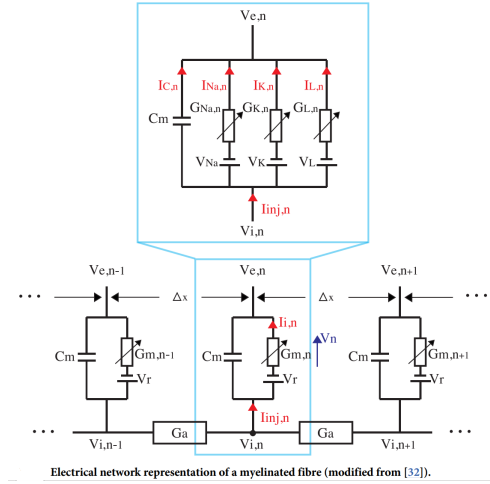
This in-depth summary of our literature research has covered how it is possible to create a nerve impulse using electrical stimulus, the feasibility of selectively activating different types of nerve fiber, the need for a biphasic input wave in order to balance the charge, and the justification for using a current source due to variable impedance of the skin. Based on this literature review, in order to function, our system needs to provide a constant current in a biphasic pattern across the electrodes.

Depth of mechanoreceptors and diameter of nerve axons in human fingerpad)

	Depth (mm)	Diameter( $\mu\text{m}$ )[13]
Meissner(RA)	0.7	3~5
Merkel(SAI)	0.9	7~12
PC(Pacinian)	2.0~	5~13



(a) This figure depicts the depths of three of four types of nerve fiber responsible for the sensation of touch. By varying the signal, it is possible to selectively activate different nerves based on their depth. If all nerves can be activated independently, any texture can be replicated [6].



(b) This is an electrical model of the membrane of the axon of a nerve. At rest, a 70mV potential drop is maintained across the membrane by ion concentration gradients. For an nerve impulse to propagate along the membrane, a voltage drop travels along the length of the nerve by opening ion channels represented by  $G_{Na}$  and  $G_K$ . An ionic current flows through the channels, creating the voltage waveform depicted in Figure 8 called an action potential. The action potential travels through the nervous system to the brain [1].

Figure 7: Nerve cell models, by depth and type and membrane electrical model.

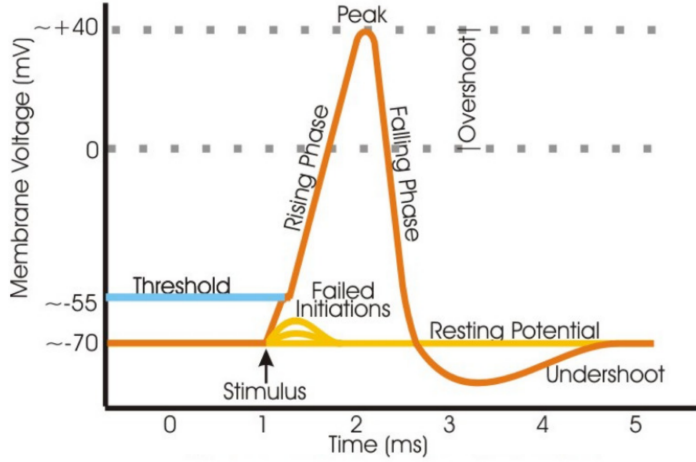


Figure 8: This is the waveform of an action potential. The y axis is the potential drop across the membrane, depicted in Figure 7(b). Resting at -70mV, if the drop is reduced beyond a threshold (-55mV) a chain reaction is activated and the rest of the waveform is generated and travels along the axon. In order to induce this excitation, we need to increase the extracellular voltage by 15mV, depolarizing the membrane [6].

### 3.1.2 Array Resolution Parameters

Our repository for system requirements originally stated a 1mm resolution of electrodes, meaning that they would be spaced 1mm apart to enable the simulation of textures as finely as 1mm apart. This was essentially a baseless number because we don't know the resolution the finger can distinguish. Very fine textures are perceived temporally, not spatially, so simulating a texture like silk would actually depend on varying the frequency of nerve activation, not by having a very spatially fine stimulus.

Since the ultimate goal is to create a realistic sensation of texture, the best method to find the optimal spatial resolution would be through testing. We could conduct a series of tests using arrays with different electrode spacing. We could then determine at what point the user can no longer tell a difference, finding exactly what spatial resolution is necessary to achieve maximum realism.

For our proof of concept prototype, we deviated from the 1mm specification up to 4.33mm because of the fabrication challenges we faced. We also lacked the means to create such

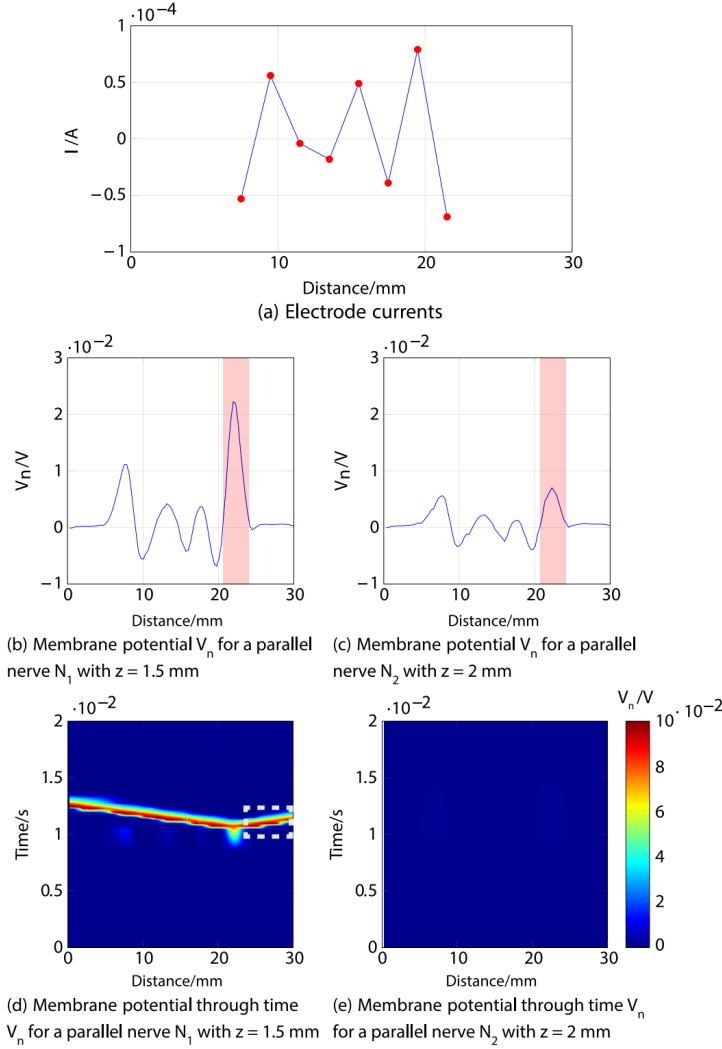


Figure 9: Illan et. al. find that they can selectively activate  $N_1$  (b, d) without activating  $N_2$  (c, e) using the current pattern depicted in a. This demonstrates that by modulating the waveform and pattern of the stimulus current, it is possible to control the activation of different nerves and reproduce any texture that is normally detected by these nerves. [1].

a fine electrode array. Since the aforementioned resolution optimization test relies on the completion of the minimum viable product, the deviation from our original spec was not a significant setback. The current dimensions of our array are depicted in Figure 11. The 3D printed piece that holds the electrodes in place is depicted in Figure 25 in the Appendix.

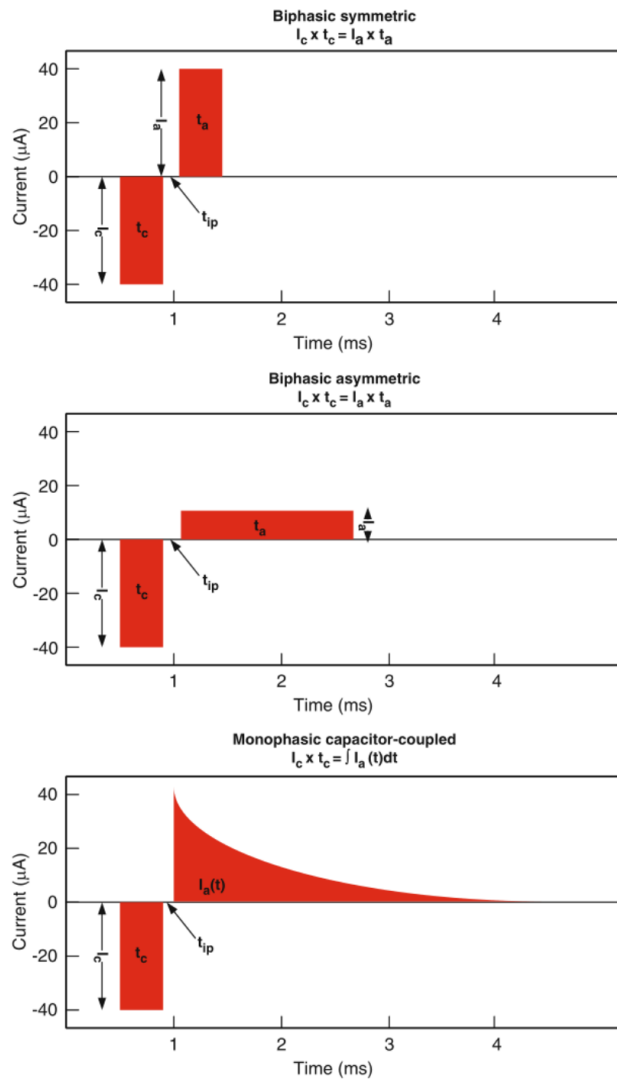


Figure 10: This figure depicts several methods for balancing the charge across the electrode. It is necessary for the positive and negative areas to be equal in order to prevent ionic accumulation at contact points as well as to reduce the rate of redox reaction in the electrode material which can improve electrode lifespan [2].

### 3.1.3 Array Parasitic Capacitance Modelling

A potential issue arises from arrays of electrodes spaced very close to each other. The electrodes will form capacitors based on their proximity and the equation for a parallel plate capacitor:  $C = \epsilon \frac{A}{d}$ , where  $C$  is the resulting capacitance,  $\epsilon$  is the dielectric constant of the insulator between the electrodes (in our case 3D printed PLA for which  $\epsilon = 3.2$ ),  $A$  is the area of the plates facing each other, and  $d$  is the distance between electrodes.

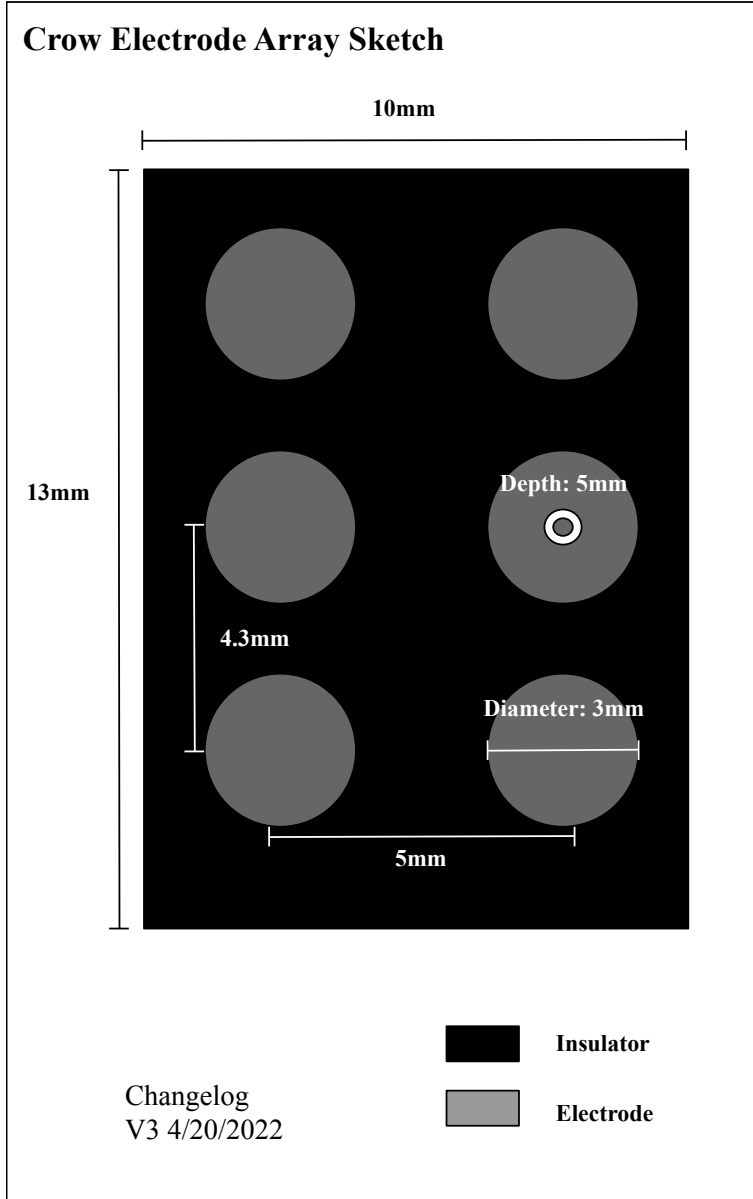


Figure 11: This figure shows the dimensions of the electrode array and each electrode. Tolerance is  $\pm 0.5\text{mm}$ .

Based on the geometry of the electrodes, the dielectric of PLA, and the distance between electrodes calculated using the following integral:  $\int_{-r}^r (D - 2r) + 2(r - \sqrt{r^2 - x^2})dx$ , we found the theoretical capacitance between each electrode pair. These values are depicted in the diagram, Figure 12.

We measured the real capacitance between electrodes using a multimeter and an oscilloscope and found it to be around 18pF. This value is much higher than the calculated

several hundred femtofarads. We found this to be due to the capacitance between the wires coming from the array. We could separate the wires to reduce the capacitive coupling, but a PSpice analysis of the frequency response of the parasitic capacitors showed a very high corner frequency, around 100kHz depicted in Figure 23. We are not even capable of driving our circuit to frequencies this high, nor would we want to so we saw no need to separate the wires. That said, one of our approaches to improving stimulus discussed in Section 3.2.3 *does* involve increasing the frequency of the signal. Although we were only able to reach 10kHz, with upgraded components it is possible we could approach the corner frequency and lose some of our signal through the parasitic capacitance.

There are a few strategies we could use to reduce the capacitance if it became an issue: one is to detach the wires from each other and route them along the glove. If the electrode capacitance was a issue we could redesign them to be thinner, which would dramatically reduce the capacitive coupling. If we were to redesign the electrodes to be closer together, this would increase the capacitance as well. We would have to ensure the new electrodes minimize their parallel area in order to minimize the coupling.

### 3.1.4 Array Material Selection

We chose the material primarily based on availability and cost. In professional applications, irridium and irridium oxide electrodes are often used due to their resistance to redox reactions and corrosion. Unfortunately irridium is outside of our budget. We chose to use titanium electrodes. Their light weight is an advantage, and we were able to source a thin titanium rod that made the electrode fabrication process manageable with the tools we had access to. The Pugh chart used to inform this decision is depicted in Figure 13.

For a final product we would want to more carefully consider the electrode material and

### Array v3 Electrode Capacitance States

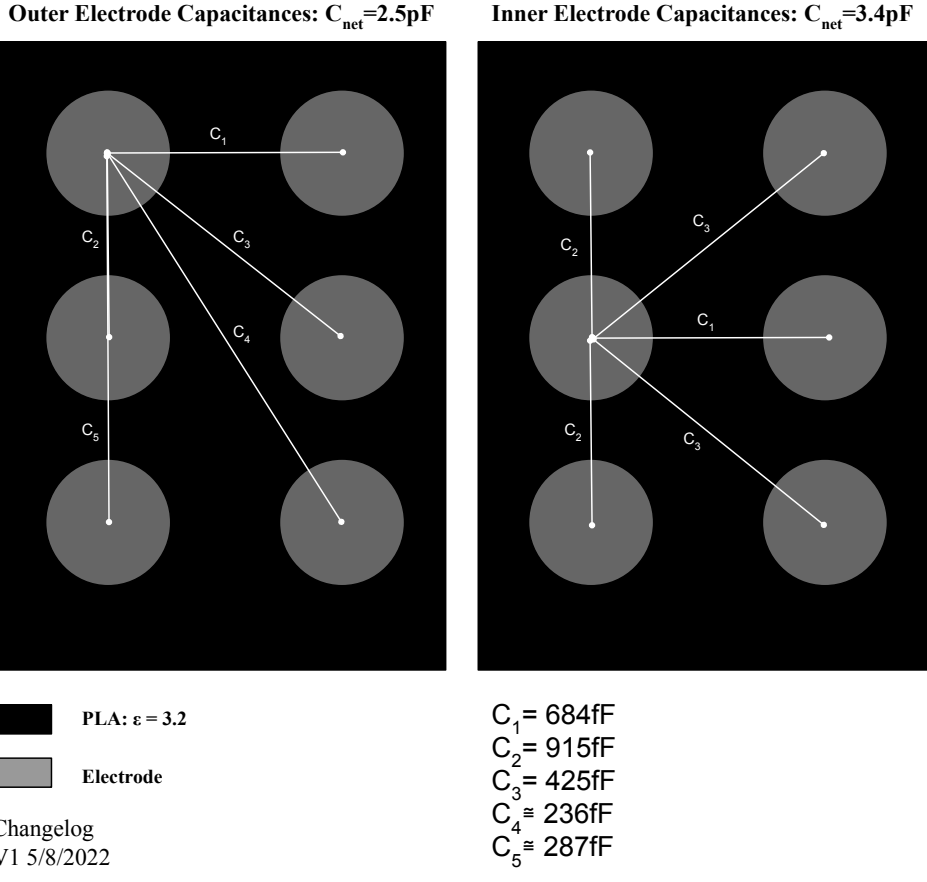


Figure 12: This figure shows the calculated theoretical capacitances between each electrode pair. Calculations are described in section 3.1.3.

fabrication process. We are still unlikely to use iridium to keep the cost of the final product low. An important parameter for electrode material selection is roughness factor [2]. This is the ratio of geometric surface area to real surface area. While the geometric surface area of an electrode can be calculated easily, the real surface area depends on the roughness of the electrode which affects how much skin is actually in contact with the electrode. With a rough electrode, the real surface area could be greater than the geometric surface area by a significant margin. Although we lacked the tools and expertise to measure roughness and our electrode suppliers did not have the information available, it must be taken into account for the final product.

## Electrode Material Pugh Chart

Option	Price	Availability	Fabrication	Durability/Reactivity
Titanium	+	+++	++	+
Stainless Steel	+	+++	++	+
Iridium/Iridium Oxide	----	-	--	+++
Titanium Nitride (Coating)	----	-	+	++
AgCl	---	+	-	++
Weight	3	3	2	1

We choose to go with titanium or stainless steel for these prototypes. These are far cheaper and easier to turn into an array. They might not be optimal in terms of performance and resistance to corrosion, but the cost and availability offsets that weakness.

V3 4/19/2022

Figure 13: Electrode Material Selection Pugh Chart.

### 3.1.5 Potential New Strategies/Designs

Throughout the year we spent working on the project, it has become clear that not only is the electrode array critical to the goals we have for a final product, but also that our prototype version is a far cry from a marketable product. Though it serves its purpose in the proof of concept, we have devised a new strategy for a superior setup.

One of the main problems with the current version of the array is its size and rigidity. If scaled to cover the whole hand it would severely compromise the ergonomics of the glove. An array with no solid mounting substrate would circumvent this issue. A new electrode, designed to be sewn directly into the fabric of a glove or other garment would unlock the true ergonomic potential of the electrode haptic system. Some potential issues that arise from this include the new requirement of a very snugly fit garment in order to maintain contact with the skin. The cloth folding could also present the risk of shorting electrodes. If these problems solved, the cloth array would be the ideal solution for optimizing ergonomics and scalability.

## 3.2 Signal Driving Circuit

### 3.2.1 Establishing Signal Requirements

The signal required for electro-tactile stimulation has been the topic of many research papers. During our examination of prior art, several of these papers were thoroughly reviewed to inform the requirements of our final trans-electrode signal. There were many factors to consider but there were two basic characteristics required before our own testing could be conducted.

We have already explained in Section 3.1.1 that the signal must be symmetrically biphasic to best minimize natural redox reactions. In addition to this, a prevailing theme amongst all the reviewed papers established the necessity of controlling the current flowing through the fingertip [5], [7], [3]. This means maintaining a constant current between electrodes forcing voltage to be the impedance dependent variable. This was done in order to prevent the wide variations in electro-bioimpedance of the skin from affecting the intended perceived signal. The reason for this is also described in Section 3.1.1. With the basic requirements of a symmetrical biphasic signal as well as a constant current established, the rest of the possible final signal parameters were left as variables so we could experimentally optimize them to maximize the realism of simulated textures.

One paper described achieving the maximum perceptible range with their signal comprised of groups of three  $40 - 100\mu s$  pulses repeating at  $200Hz$  and being gated into bursts repeating at  $50Hz$  [5]. This same paper states that a voltage range of  $150 - 500V$  is required but voltages over  $350V$  caused electrical arcing as a finger neared the electrode. This was described as painless but seemed undesirable, so we defined our goal supply voltage for the driving circuit to be in the range of  $150V - 350V$ . With a circuit outputting a constant current, it will adjust the voltage to exactly as much as is necessary to drive the commanded current through the impedance, within the limits of the supply voltage.

The supply voltage now determines the maximum resistance we can provide with our desired signal. It was also described that the fingertips generally require a lower current ( $1 - 10mA$ ) and higher voltage ( $150 - 500V$ ) when compared to other parts of the body. Less current is required because of the greater density of touch sensing nerves yet a higher voltage is required because of the thickness of the skin in the area. Skin resistance was estimated by them to be approximately  $150k\Omega - 300k\Omega$ .

A paper reviewed later described the threshold voltage for perceiving stimulus could be as low as  $10V$  with needle electrodes [7]. The paper also experimented with different frequencies and duty cycles to determine the lowest threshold voltage on their setup was achieved with a 35% duty cycle,  $100Hz$  signal. This signal was perceptible with a mere  $58V$  supply. The current they utilized was not defined in their paper but the integrated circuit they claimed to be using, the HV507 chip has a maximum current output of only  $1mA$  [8].

Armed with this information, we knew for certain that our wave driven across electrode pairs must be a constant current of adjustable amplitude and we must have the ability to switch between positive, negative, and zero output. Figure 14 shows a graphical representation of the target signal. Each labeled variable should be controllable in the output of the driving circuit.

The amplitude of the current should be capable of reaching anywhere in the range of  $1 - 10mA$ . The voltage supply should allow for  $300V$  ( $\pm 150V$ ). The circuit should also be capable of switching polarity with at least the speed for pulse widths as short as  $1750\mu s$  at the maximum voltage. Pulse widths of  $1750\mu s$  for positive then negative pulses, allows for a 35% duty cycle at  $100Hz$ .

## Target Driving Wave

(as measured across a cathode and anode electrode pair)

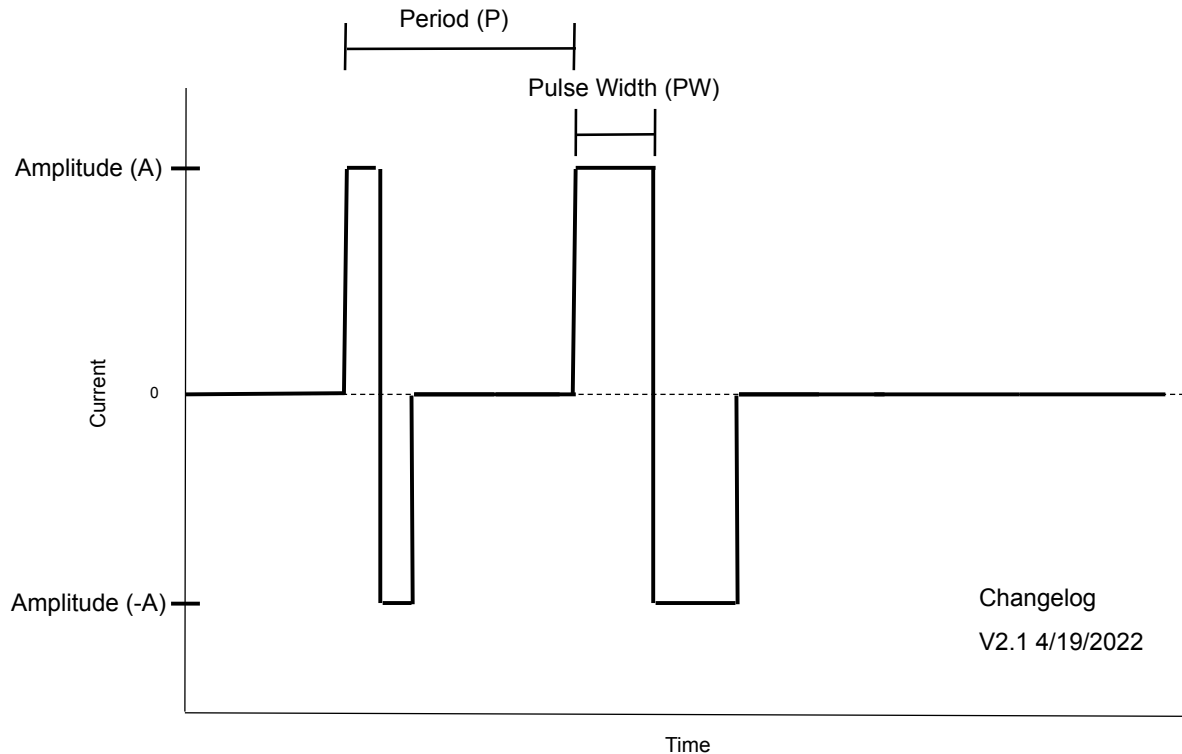


Figure 14: Goal signal across electrode pairs with variables represented in parentheses.

### 3.2.2 Converting Microcontroller Signals to Meet Requirements

With the basic signal requirements between each cathode and anode electrode pairs established, the driving circuit must implement these requirements using the microcontroller. This is necessary to make the final stimulus software-controllable for Virtual Reality simulation. The vast majority of microcontrollers can output a signal of 0V OR 3.3V with their General Purpose Input Output pins (GPIO). With an onboard Digital-to-Analog Converter (DAC) the signal is able to hit points in the range 0 – 3.3V (sometimes 0 – 5V) depending on the resolution. The microcontroller we chose for our minimum viable product (decision detailed in Section 3.3) is capable of hitting our signal speed requirements but required some way to turn the monophasic signal into a biphasic sig-

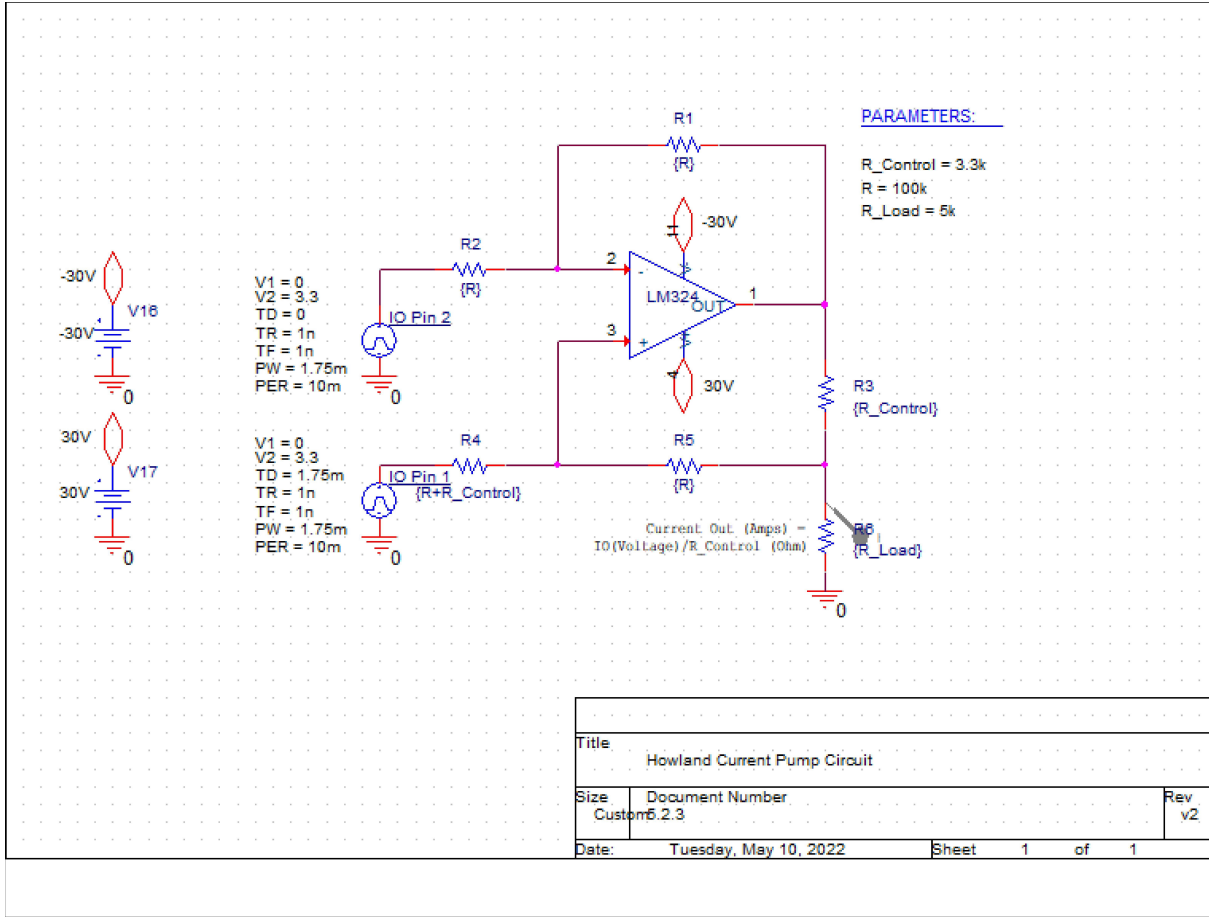


Figure 15: Schematic of our most updated circuit.

nal. We also needed a way to turn the constant voltage with a load dependent current into a constant current with a load dependent voltage.

Both these requirements were satisfied with the circuit schematic in Figure 15.

A study published by Texas Instruments, stated that the ratio between  $R_1$  and  $R_2$  determines the gain of the op-amp [3]. We kept the ratio at 1/1 throughout our testing. The value of  $R_1$ ,  $R_2$ ,  $R_5$ , and the non-control part of  $R_4$  were kept at  $100k\Omega$ . The study stated that the  $R$  resistance must remain high enough to drop the voltage at the operating current that is feeding to the op-amp.

This current out is determined by the relationship  $I_{out} = \frac{V_{IO}}{R_{Control}}$ . For testing purposes,

$R_{Control}$  was implemented with two potentiometers to allow for amplitude adjustment. Because the chosen microcontroller only has one onboard DAC, the IO pins were used to implement the signal. The IO pins are only capable of  $0V$  or  $3.3V$  output which means the microcontroller cannot control the final current amplitude with this circuit.

This circuit not only implements a constant current but also allows for the swapping of signal polarity across the output  $R_{Load}$  resistor. Setting  $IO\ Pin\ 1 = 3.3V$  and  $IO\ Pin\ 2 = 0V$  results in a positive constant current  $I_{out}$  across the output  $R_{Load}$  resistor. Switching to  $IO\ Pin\ 1 = 0V$  and  $IO\ Pin\ 2 = 3.3V$  results in an equal and opposite constant current output. Figure 16 details the relationship between the IO Pin inputs and the current observed across the electrodes.

With both pins set to the same voltage, either both =  $0V$  or both =  $3.3V$ , the output signal equals  $0A$ .

### 3.2.3 Voltage and Frequency Limitations Encountered

Two main issues are posed by this circuit. Because the output is powered by the op-amp, we are limited to the supply voltage and the slew-rate of op-amp we use. In the schematic (Figure 15) and in our initial testing of the circuit, we utilized the LM324N integrated circuit from Texas Instruments. This op-amp chip has a relatively high maximum supply voltage of  $\pm 32V$  but a rather low slew rate of  $0.5V/\mu s$  at unity gain [4]. The maximum supply voltage high compared to the other chips we own but it is no where near the  $300V$  ( $\pm 150V$ ) we stated as a goal in Section 3.2.1. As a result, the physical circuit in Figure 15 failed to produce a distinguishable signal. We identified three possible methods to achieve a distinguishable signal. The first was to implement the circuit using an op-amp with a supply voltage rating of  $\pm 150V$ . We identified a potential candidate integrated circuit: the PA08 from Apex Microtechnology. In addition to the high supply voltage rating, this chip has a much higher slew rate of  $30V/\mu s$  [9].

# Target Wave in Relation to IO Pins

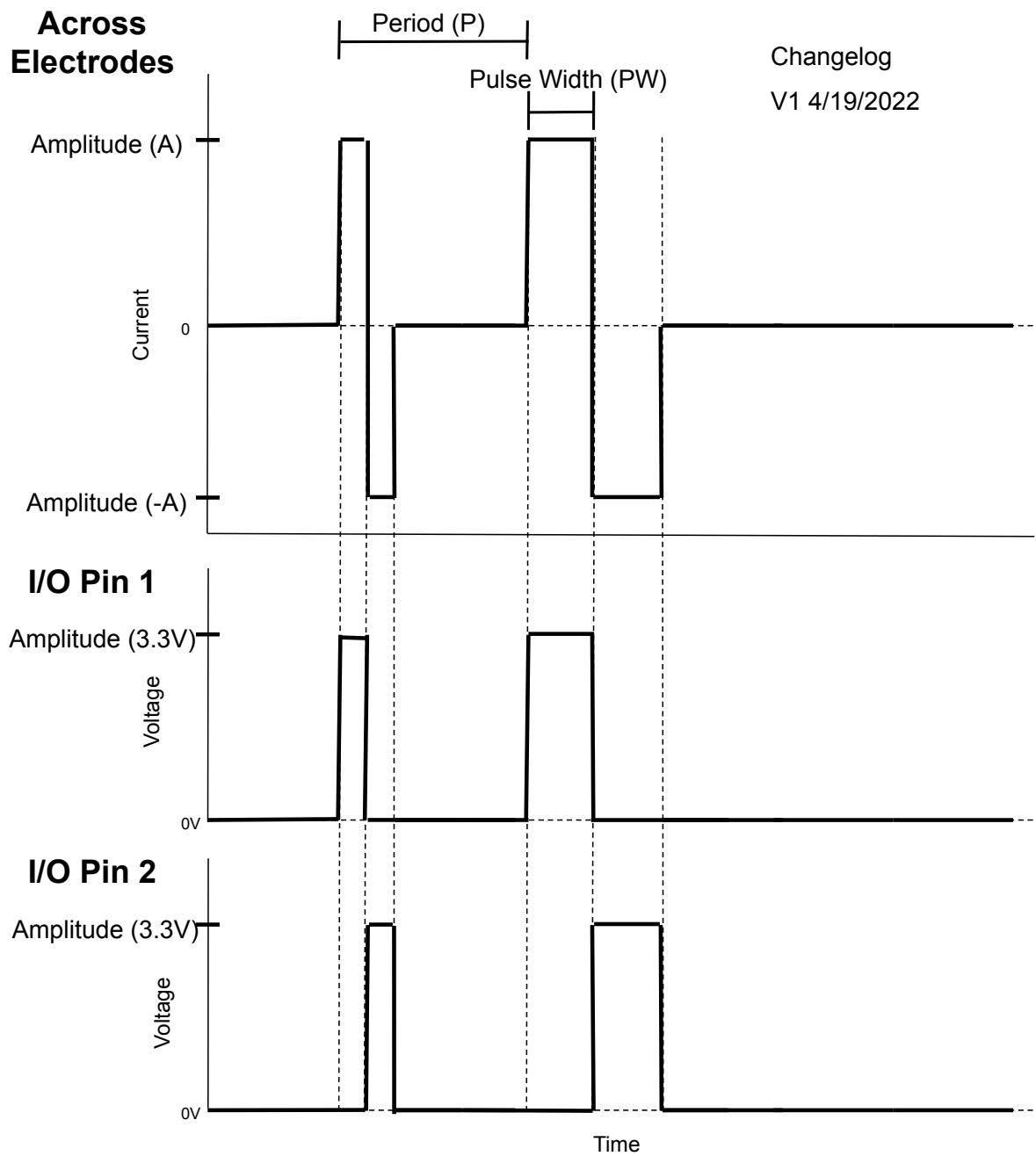


Figure 16: Relationship between IO Pin signal and the output current wave measured across an electrode pair.

Another potential method identified was to lower the minimum voltage threshold by raising the signal frequency to lower the impedance of the capacitive element in the RC skin electrical model. The details of how this signal was implemented are found in Section 3.3.

For each of our physical tests, the  $R_{Control}$  resistors which control the output current were set to  $3.3k\Omega$  resulting in output current:

$$I_{out} = \frac{V_{IO}}{R_{Control}} = \frac{3.3V}{3300\Omega} = 1mA.$$

Because the output voltage is a variable dependent on the load impedance, a test load was placed in order to measure the output voltage. With the output current tested at  $1mA$ , a load impedance was placed on the output to ground just as in Figure 15. The value was  $R_{Load} = 10k\Omega$  to give us a voltage drop of:

$$V = IR = 1mA * 10k(\Omega) = 10V$$

The  $10V$  output was set arbitrarily (the AD2 is not capable of  $30V$ ) for measuring our frequency limitations on the oscilloscope. The  $\pm 10V$  or  $20V$  swing with  $0.5V/\mu s$  slew rate meant it would take  $40\mu s$  to settle at each commanded voltage. This can be observed in Figure 17.

Because the signal is too small to be perceived at the finger tip, we are unsure if this  $0.5V/\mu s$  slope has any affect on the goal stimulation. As we are using  $30V$  in human testing, know that the slew rate will not allow the output to reach  $30V$  at  $10kHz$  (the waveform would be fully triangular). It is likely that the slope compromises the stimulus as it reduces the total current applied per pulse. It can be observed in Figure 18 that the waveform completely breaks down when commanded to  $30kHz$ . The signal is no longer symmetric.

With the supply voltages at the maximum  $\pm 30V$  of our LM324N op-amp, cycling through various frequencies from  $285Hz$  through to the slope limited  $10kHz$  still did not achieve

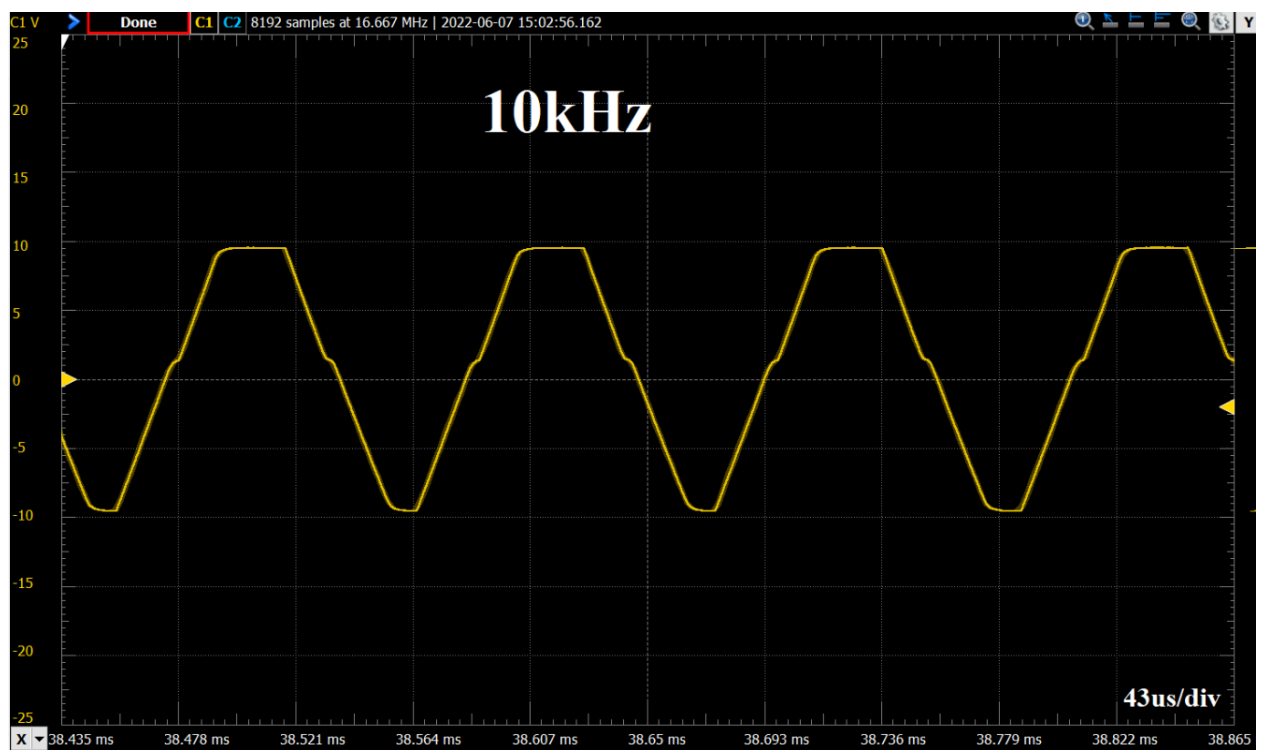


Figure 17: Slew rate limitation. The 20V swing takes  $40\mu s$  to achieve, resulting in a noticeable slope.

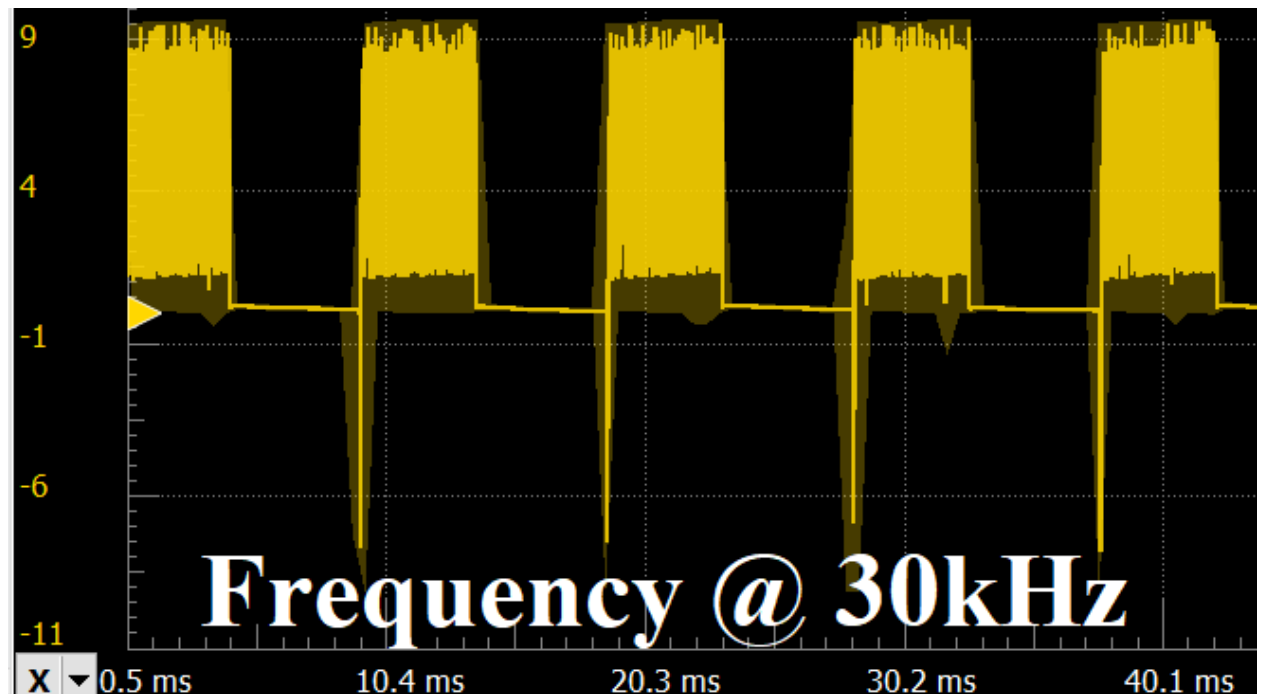


Figure 18: Complete breakdown of the waveform when set to  $30kHz$ .

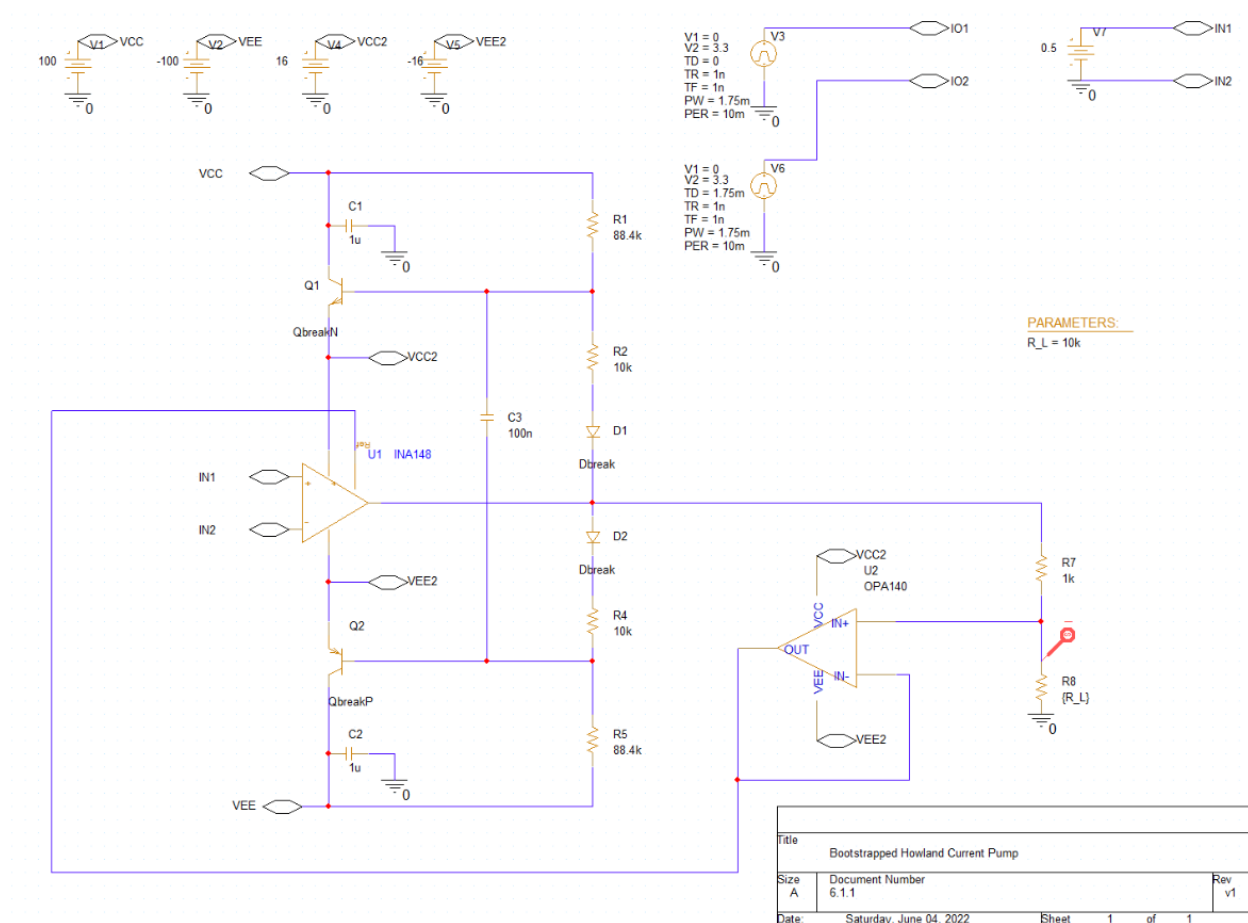


Figure 19: Bootstrapped Howland Current Pump Schematic.

a perceptible signal.

The final method of raising our output voltage involved recreating the circuit. Through further research we found a circuit known as the Bootstrapped Howland Current Pump which uses BJTs to increase the supply voltage without relying on the limits of the amplifier integrated circuit. This circuit was built in simulation as shown in Figure 19. For this circuit we would have liked to build and test it physically, but did not have a difference amplifier on hand. The circuit was discovered too late in the year to be able to buy the INA148 and have it arrive on time.

### 3.3 Microcontroller

The microcontroller subsystem will have many more responsibilities in the final consumer product than it does in the proof of concept. The features to be implemented in the final consumer product are outlined in the Repository for System Requirements (Figure 28 and will be touched on in Section 5. This section will focus on what was used to test the basic stimulus and how it was implemented.

The Microcontroller Unit (MCU) we used in our prototype is the TeensyLC. This MCU was picked because of its ease of acquisition and it's small form factor. The Pugh chart used to inform this decision is depicted in Figure 27 of the Appendix. When we first started our work, we were unsure of specifically what features would be necessary so we focused on UART, PWM, DAC, and GPIO pins. Our current implementation with the circuit in Figure 15 only requires two IO pins per electrode pair, each outputting  $1750\mu s$  duration impulses. Switching the HIGH/LOW states of the two IO pins creates the desired biphasic waveform, as shown in Figure 16. By setting the duration of these states, the microcontroller can control the period and pulse width of the target wave.

The microcontroller code was setup for the purpose of driving the signal with a variable frequency while maintaining the original waveform with a duty cycle of 35% at  $100Hz$ . By cycling through different frequencies at the press of a button, the task of testing our op-amp's limits experimentally was made significantly easier. The code for cycling through frequencies is included in the Appendix. This function also allowed for directly setting a specific frequency if requested. Maintaining the duty cycle of 35% at  $100Hz$  meant that the output current must remain high for  $\frac{3500\mu s}{2} = 1750\mu s$  and negative for an equal amount of time. The current output would then stay at zero for the remainder of the  $10ms$  period. Half of the 35% duty cycle is spent with positive output and the other half negative; this achieved our symmetric biphasic waveform.

Inside of the 35% duty cycle, because the pulse switches from positive to negative with a period of  $3.5ms$ , the frequency of within the pulse was calculated to be:

$$\text{Frequency } (f) = \frac{1}{\text{Period}(T)} = \frac{1}{3.5ms} = 285.7Hz$$

When the duty cycle was divided into 2 more sections, the frequency would be effectively doubled. Dividing into three subsections would triple it. The following simple equation was utilized to find the number of subdivisions of signal necessary to implement various different frequencies:

$$\text{Frequency } (f) = \frac{\text{Number of Divisions}(n)}{\text{Period}(T)} \longrightarrow n = f * T$$

An example of the output signal with subdivisions ( $n$ ) = 3  $\longrightarrow f = 857.1Hz$  can be seen in Figure 20.

### 3.4 Glove Design

The glove is the least essential subsystem in the context of our proof of concept design. It is not strictly necessary for the main goal of producing a distinguishable stimulus. We still developed the prototype glove in order to convey our vision of the final product. Unlike the proof of concept, for the final consumer product the high standard for comfort and ergonomics will make the glove a critical subsystem. Our prototype glove is pictured in Figure 21.

The most useful part of the prototype glove is the finger mount, a 3D printed part designed in Solidworks that holds the electrode array and has an opening for the finger. This keeps the array tight to skin to ensure good contact and was useful for testing. It is pictured in Figure 6(a). The engineering drawing for the finger mount is in Figure 22.

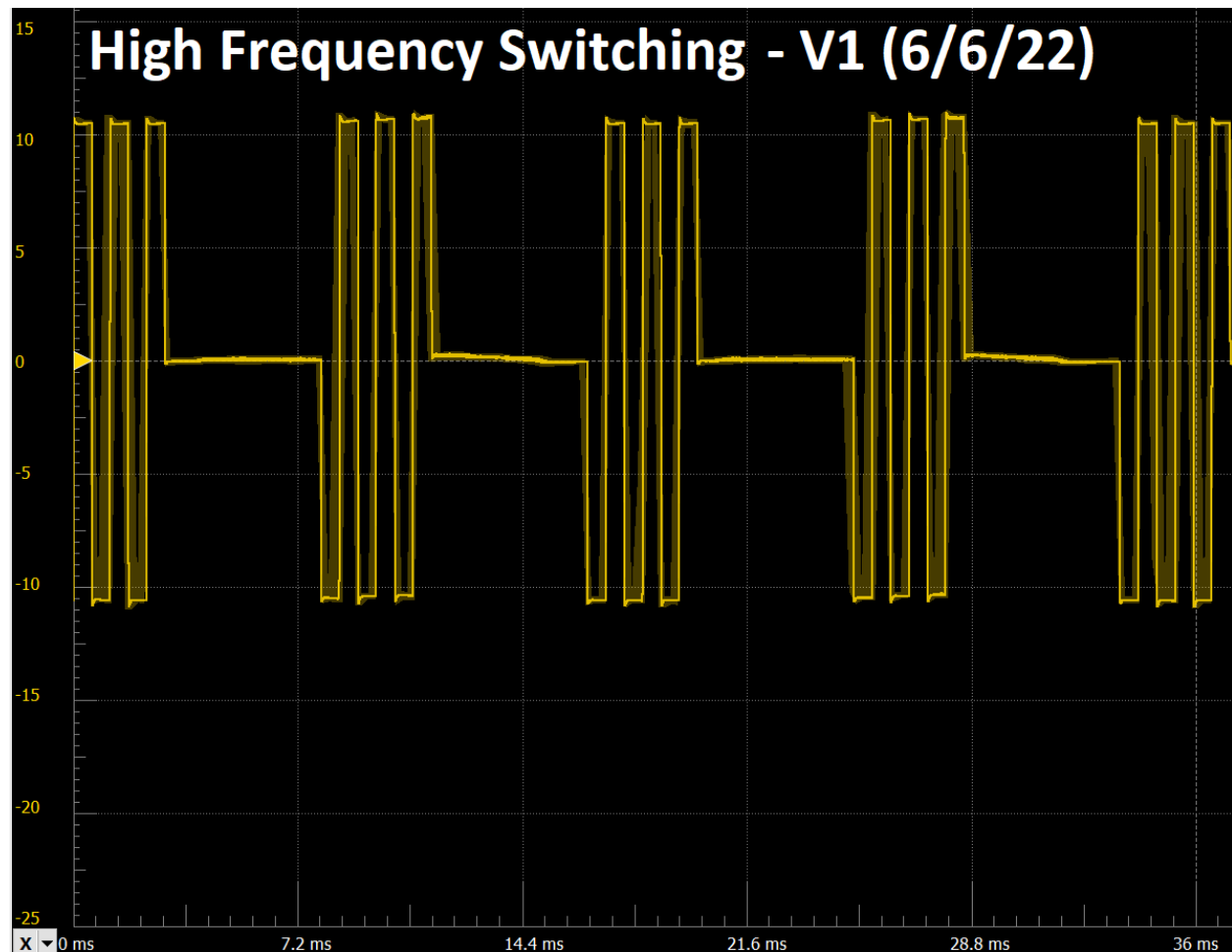


Figure 20: Example of active duty cycle subdivided into 3 pulses high, 3 pulses low rather than the standard 1 high, 1 low.



Figure 21: Prototype glove. Four additional <sup>32</sup> dummy array holders are included for demonstration purposes, but hold no electrodes.

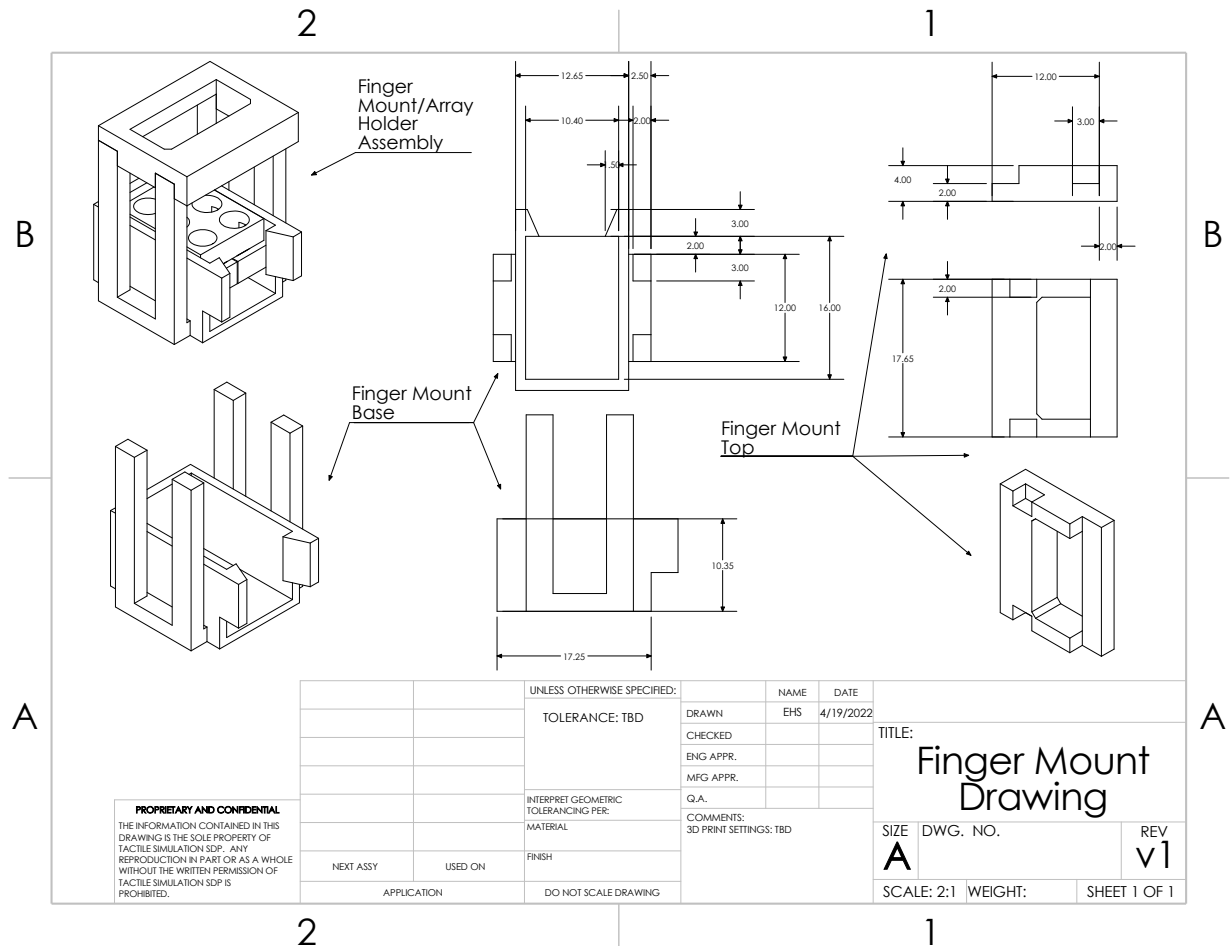


Figure 22: Engineering drawing of the finger mount component of the glove. Tolerance is  $\pm 0.1\text{mm}$ .

## 4 Mistakes Made and Subsequent Lessons Learned

One of the most valuable lessons we've learned over the course of this past year is the importance of task planning. Inadequate task planning at the start of the year seemed to make our small amounts of progress futile. As we learned the true nature of the obstacles we were attempting to tackle, we slowly became more adept at managing our workflow. Dividing time intensive tasks into smaller segments and defining them to be more specific in scope allowed us to better anticipate the effort we would need to put into each sprint and helped us accomplish our sprint objectives. This proved es-

pecially important because of how much trial and error we went through during the project.

We started out thinking that getting a working stimulus would be a one task event but in reality we ended up spending multiple sprints trying to achieve this goal. The tasks were broken down into more narrowly focused goals such as testing specific circuits for desired results. We also learned the importance of good documentation. In the process of trying to learn from our mistakes, we developed a process of writing down everything important to our experimentation which proved valuable as we amassed information and knowledge about the project.

## 5 Next Steps

### 5.1 Our Design

As discussed throughout the report, there are numerous discrepancies between our Repository for System Requirements and our current iteration of the device.

Increased coverage, Bluetooth connection, battery power, VR integration, and texture recognition software are just a some of the features we wanted to implement. The glaring hole in our design is the failure of the proof of concept prototype. The next step of the project needs to be to complete this basic version. Once that is complete, we can look to the future and begin implementing the originally planned features.

### 5.2 Nerve Stimulation in Virtual Reality

A previously undiscussed but promising application of electrical nerve stimulation in Virtual Reality is to implement it alongside mechanical actuation in one device. Our thin electrodes can be implemented inside mechanical haptic feedback gloves capable of force feedback in order to add texture to the VR experience.

When comparing the two systems as competitors rather than working in tandem, we still believe the electrode stimulation system has significant advantages over mechanically actuated systems. It is a certainty that with the advent of brain computer interfaces in years to come that direct control over the nervous system will be the future of Virtual Reality and beyond. The question that remains is whether or not an electric stimulation system like ours will find a place in bridging the gap between our current technology and the virtual future.

## 6 Appendix

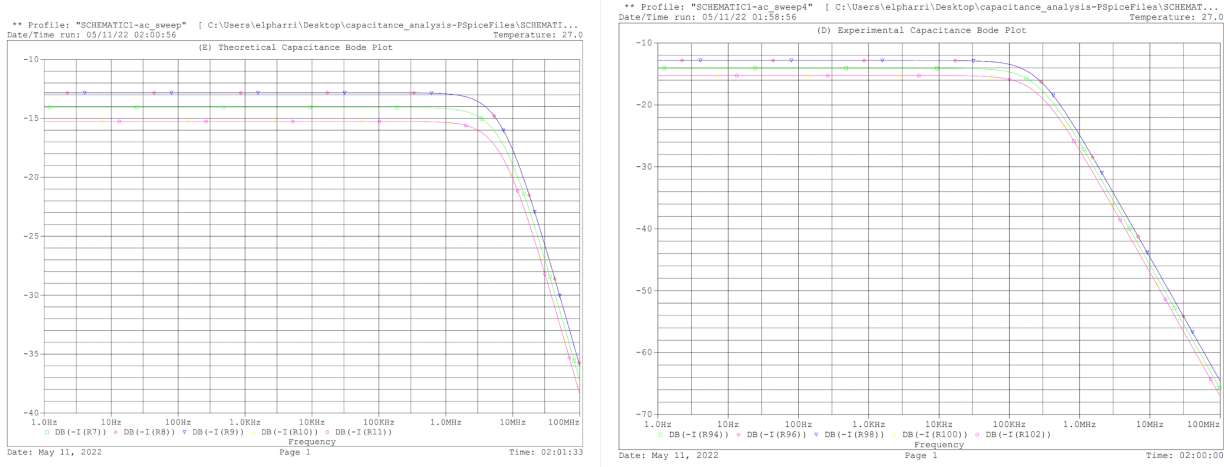


Figure 23: Bode plot of simulated frequency response of capacitive electrodes: theoretical and real models.

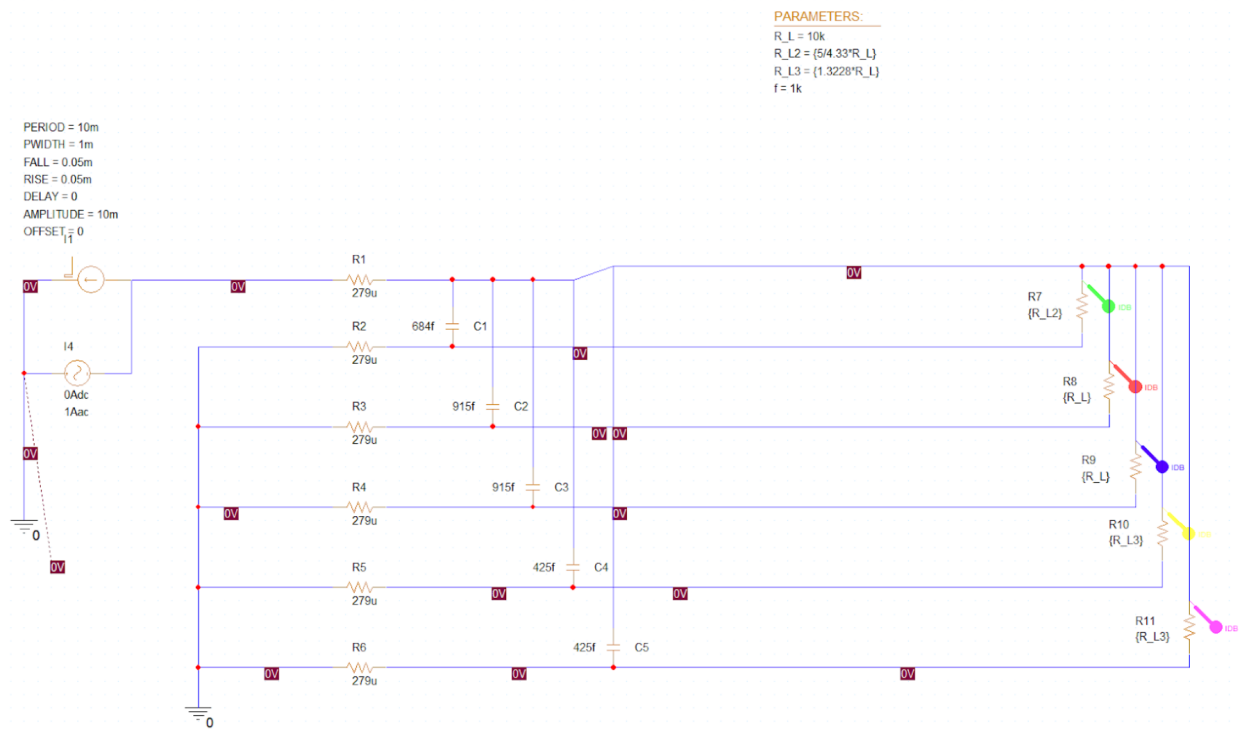


Figure 24: Circuit used to generate bode plots in Figure 23.

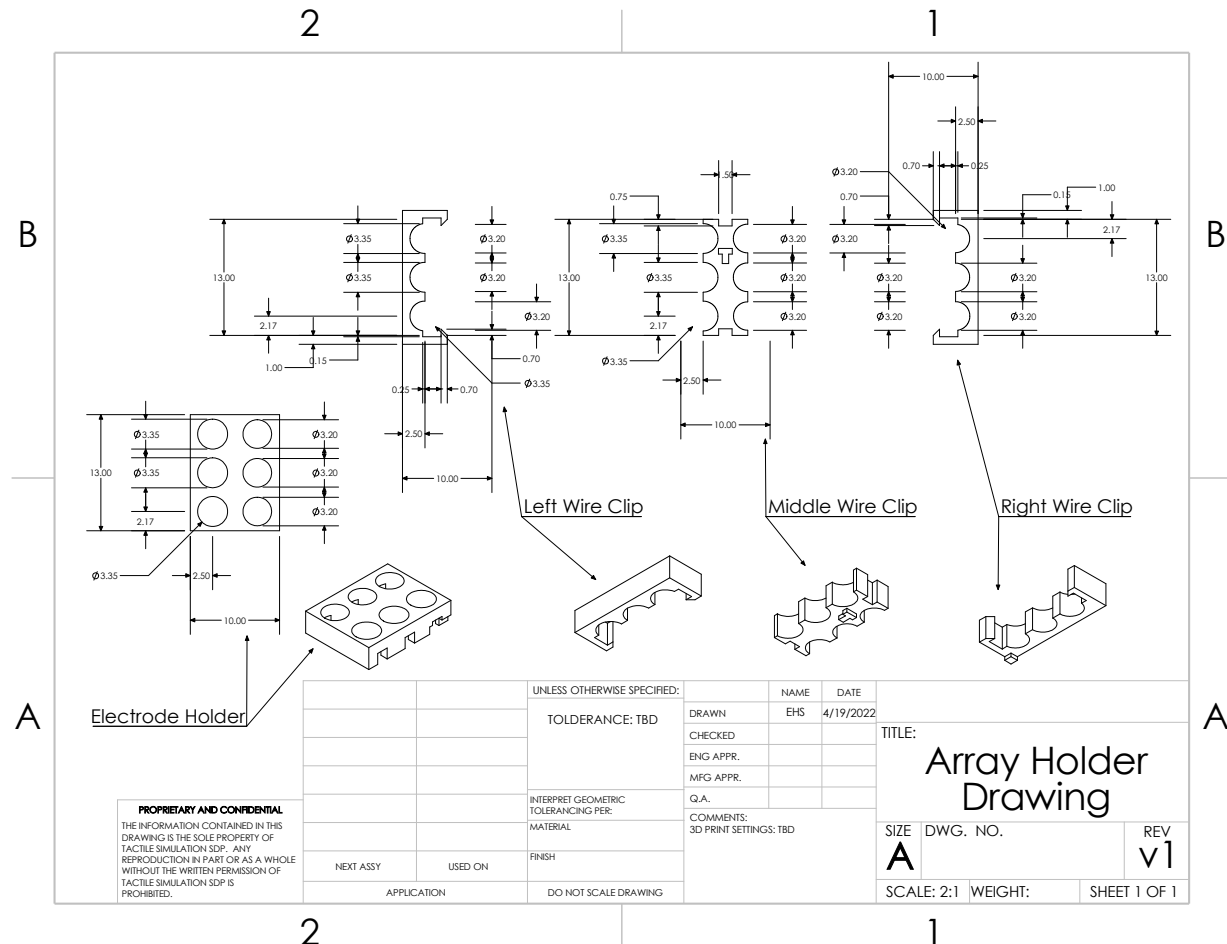


Figure 25: Engineering drawing of the array holder. Tolerance is  $\pm 0.1\text{mm}$ .

```

1 ///////////////////////////////////////////////////////////////////
2 // Created by Jacob Sickafoose on 4/16/22 // 
3 // Updated for the Final Prototype // 
4 ///////////////////////////////////////////////////////////////////
6 #include <Arduino.h>
7
8 ///////////////////////////////////////////////////////////////////
9 // PUBLIC # DEFINES //
10 ///////////////////////////////////////////////////////////////////
11 #define buttonIn 4 // Defines the button input pin as 4
12 #define period 10000 // Frequency of signal in microseconds

```

```

13
14 #define IO_1 16      // Defines two IO pins switch the H-Bridge for pair 1
15 #define IO_2 19      // pair1.pin1 and pair1.pin2 corresponding to pin 10 and
16   11 on the board
17
18
19 ///////////////////////////////////////////////////////////////////
20 // PRIVATE # DEFINES //
21 ///////////////////////////////////////////////////////////////////
22 #define LED LED_BUILTIN // Gives the LED a better name
23
24 ///////////////////////////////////////////////////////////////////
25 // PRIVATE Variables //
26 ///////////////////////////////////////////////////////////////////
27 elapsedMicros usec;           // Creates microsecond timer variable
28 elapsedMillis milli;
29
30 uint16_t LED_Delay = 0;
31 uint8_t timerMode = 0;         // Stores the flipflop for IO pins to swap
32   positions in time
33 uint8_t LED_ON_FLAG = 0;
34 int IO_Duty = 0;              // Stores delay number for IO
35 int Off_Delay = 0;
36 uint16_t subdivisions = 1, counter = 1;
37 uint8_t pinChange = 1;
38
39 ///////////////////////////////////////////////////////////////////
40 // Board INIT //
41 ///////////////////////////////////////////////////////////////////
42 void setup() {
43   // Intializing Pins as Outputs

```

```

44 pinMode(LED, OUTPUT);
45 pinMode(IO_1, OUTPUT);
46 pinMode(IO_2, OUTPUT);
47
48 // Inits the buttonIn pin
49 pinMode(buttonIn, INPUT);
50
51 digitalWrite(LED, LOW);      // Inits LED as off
52 digitalWrite(IO_1, LOW);
53 digitalWrite(IO_2, LOW);
54
55 Off_Delay = period/2;
56 IO_Delay = 1750;
57 }
58
59
60
61 ///////////////
62 // MAIN LOOP //
63 ///////////////
64 void loop() {
65     // Changes the frequency if if button is pressed
66     if (!digitalRead(buttonIn)){ // If button is pressed, meaning logic LOW
67         // Display LED on
68         digitalWrite(LED, HIGH);
69
70         if (subdivisions == 4){
71             subdivisions = 35;
72         }
73         else if (subdivisions == 35){
74             subdivisions = 105;
75         }
76         else if (subdivisions == 105){

```

```

77     subdivisions = 175;
78 }
79 else if (subdivisions >= 175){
80     subdivisions = 1;
81 }
82 else {
83     subdivisions++;
84 }
85
86 // Delay by 2 seconds for some debouncing
87 delay(700);
88 }
89 else {
90     digitalWrite(LED, LOW); // LED off when it is not changing mode
91 }
92
93
94
95 // Timer for LED flashing
96 if (milli > LED_Delay){
97     milli = 0;
98
99     if (LED_ON_FLAG == 1) {
100         digitalWrite(LED, HIGH);
101         LED_ON_FLAG = 0;
102         LED_Delay = 100;
103     }
104     else{
105         digitalWrite(LED, LOW);
106         LED_ON_FLAG = 1;
107         LED_Delay = 2000;
108     }
109

```

```

110     }
111
112
113 // Code to calculate IO_Delay from subdivisions
114 IO_Delay = 1750/subdivisions;
115
116
117
118 // Timer for setting IO High/Low Values
119 // Electrode 0V
120 if (timerMode == 0){
121     if (pinChange){
122         digitalWrite (IO_1, LOW);
123         digitalWrite (IO_2, LOW);
124         pinChange = 0;
125     }
126     if (usec > Off_Delay){
127         usec = 0;
128
129         timerMode = 1;
130         pinChange = 1;
131     }
132 }
133 // Electrode HIGH
134 if (timerMode == 1){
135     if (pinChange){
136         digitalWrite (IO_1, HIGH);
137         digitalWrite (IO_2, LOW);
138         pinChange = 0;
139     }
140     if (usec > IO_Delay){
141         usec = 0;
142

```

```

143     timerMode = 2;
144     pinChange = 1;
145 }
146 }
147 // Electrode LOW
148 if (timerMode == 2){
149     if (pinChange){
150         digitalWrite(IO_1, LOW);
151         digitalWrite(IO_2, HIGH);
152         pinChange = 0;
153     }
154     if (usec > IO_Delay){
155         usec = 0;
156
157         if (counter < subdivisions){ // Now the counter determines if it goes
158             HIGH again or goes back to 0V state
159             timerMode = 1;
160             counter++;
161         }
162         else{
163             counter = 1;
164             timerMode = 0;
165         }
166         pinChange = 1;
167     }
168 }
169 }
```

Figure 26: Final C code implementation for switching frequency.

## Decision Parameters

- **Ease of acquisition**

This parameter is key for our first prototype seeing as our requirements are much more simple and our goal is to quickly achieve a working proof of concept. Two of these chips are already owned by us, meaning the ease of acquisition score is extremely high. On the opposite end, a hard to acquire microcontroller might be one that is not mass manufactured, or would have a long shipping time. Somewhere in-between would be buying from BELS or the internet with a quick shipping speed.

- **DAC Output pins**

For our first prototype, it is mandatory that our microcontroller has at least one DAC. For the future prototypes, having more might be handy but it remains to be determined. The results of our first prototype may dictate different requirements. All of these boards include at least one digital to analog converter.

- **PWM Output pins**

Our microcontroller must have at least one PWM pin for similar reasons as the DAC. We only need one for now, and more may be unnecessary. Because most microcontrollers do have a PWM pin, it is not a large factor. If a microcontroller did not have an onboard DAC, we would be able to make do with PWM low-pass filtering to generate a wave for our electrode.

- **Onboard Bluetooth**

Onboard bluetooth is not completely necessary because of the availability and ease of use of external bluetooth breakout boards. Especially for our first prototype where we will not be utilizing bluetooth. It would however be a welcome addition to our board, so long as it supports HID and SPP bluetooth profiles so we can properly communicate with the host device.

- **UART Capability**

The vast majority of microcontroller options already had UART capabilities, but it is fair to say that it is still an absolute necessity for our project. Multiple will not be helpful, but at least having one was mandatory.

- **Price**

The price is not going to be much of a concern until our final device, because that's when we can strip functionality of the microcontroller down to the bare minimum to push our electrodes. Of course, already owning the microcontroller is a positive for the price.

- **Ease of use**

I'm confident that I can figure out how to use any microcontroller in short time. Most of them are capable of being programmed with C, which is how we coded in ECE121. It would be a benefit to use a microcontroller that we specifically already programmed before, but definitely not required. The PSoC however, seems to not be programmable in C, making it slightly lower on the ease of use scale.

**Microcontroller Comparison Table, Tactile Simulation Team (E. Harrison, J. Sickafoose)**

	Teensy LC	CY8CKIT-059 PSoC	ESP32-D0WD-V3
<b>DAC Output pins</b>	1, 12-bit	4, 8-bit	2, 8-bit
<b>PWM Output pins</b>	10	4	3
<b>Onboard Bluetooth</b>	0	0	1
<b>Processor Clock Speed</b>	48MHz	Up to 80MHz	Up to 240Mhz
<b>Flash Memory</b>	128KB	Up to 256KB	4MB
<b>SRAM</b>	16KB	Up to 32KB	520KB
<b>Digital I/O Pins</b>	27, NOT 5V tolerant	46-72, unspecified voltage	34, 5V tolerant
<b>Onboard LEDs</b>	1	0	8
<b>Analog Input Pins</b>	13, 16-bit	2, 12-bit	2, 12-bit
<b>Operating Voltage</b>	1.71 to 3.3V	1.71 to 5.5V	3.3V
<b>Operating Amperage</b>	<100mA, max	15.4mA @48MHz	30~68mA, @ 240MHz
<b>Standard Operation Power</b>	<330mW	~77mW	~100mW
<b>DC Output current</b>	<100mA	25mA	1200mA, cumulative

**Pugh Chart**

Decision Parameter	Weighting	TEENSY LC	CY8CKIT-059 PSoC	ESP32-D0WD-V3
Ease of Acquisition	4x	+++	+++	+
DAC Output Pins	3x	+	++++	++
PWM Output Pins	1x	+++++	++	+++
Onboard Bluetooth	2x	0	0	+
UART Capability	6x	+	+	+
Price	1x	+++	++	+
Ease of Use	4x	++	0	++
Totals		37	34	30

**Change Log v0.1 (1/18/22)**

- First Start with Teensy LC, CY8CKIT-059 PSoC, and chipKIT Uno32

**Change Log v1.0 (1/19/22)**

- Switched the chipKIT Uno32 to ESP32-WROOM-32D because it was more relevant to our project

Figure 27: Pugh chart and design decisions behind the microcontroller selection.

**Repository for System Technical Requirements**

	Criteria	Requirement	Type	Hierarchy	Verification	Specification
Texture Simulation	Simulated textures feels realistic	The glove shall produce a realistic simulation of texture.	Performance	Subsystem	User testing to determine realism	N/A
	Number of simulated textures	The glove should be able to simulate enough distinct textures to create an immersive environment.	Performance	Subsystem	Software review	>100 textures
	Temporal Resolution	The glove shall be capable of producing an electrical stimulus at different frequencies in intervals of 500mHz.	Performance	Subsystem	Electrode performance test	500mHz
	Spatial Resolution	The glove shall be capable of creating a stimulus with spatial resolution of 4.3mm.	Performance	Subsystem	Electrode performance test	4.3mm
	Spatial Coverage	The glove shall be able to provide stimulus on greater than 50% of the surface area it covers.	Performance	Subsystem	Hand modeling	>50% coverage
Usability	User friendly	The device shall not disconnect unexpectedly or cause discomfort during standard use.	Functional	System	User analytics on session length	N/A
		Battery shall last 3 hours	Functional	Component	Component	3 hours

	Battery Life	of constant use.			testing	
	Device connectivity range	The glove shall maintain connectivity within 3 meters of the headset.	Functional	Subsystem	Component testing	5m
	Ergonomics	The glove should be comfortable to wear for prolonged periods of time (3hr).	Functional	System	User analytics on session length	3hr (battery life)
	Device weight	The glove shall weigh 500 grams or less.	Functional	System	Component testing	500g
	Hand Fit	The glove should fit any reasonably sized hand.	Functional	Subsystem	Testing of glove fit	N/A
Durability	Durable in normal use	The glove should not be damaged from reasonable operation.	Environmental	System	In-house developed stress test	N/A
	Water/Dust Proof	The device should be resilient to exposure to water and particulate matter.	Environmental	System	Ingress Protection Test	IP57

**Change Log v0.1 (1/19/2022)**

- First draft completed

**Change Log v2.0 (4/20/2022)**

- Changes spatial resolution from 1mm to 4.3mm
  - Necessary to enable 2 dimensional stimulus

Figure 28: Repository for System Technical Requirements. Stores specifications that we have identified as critical to a complete final product.

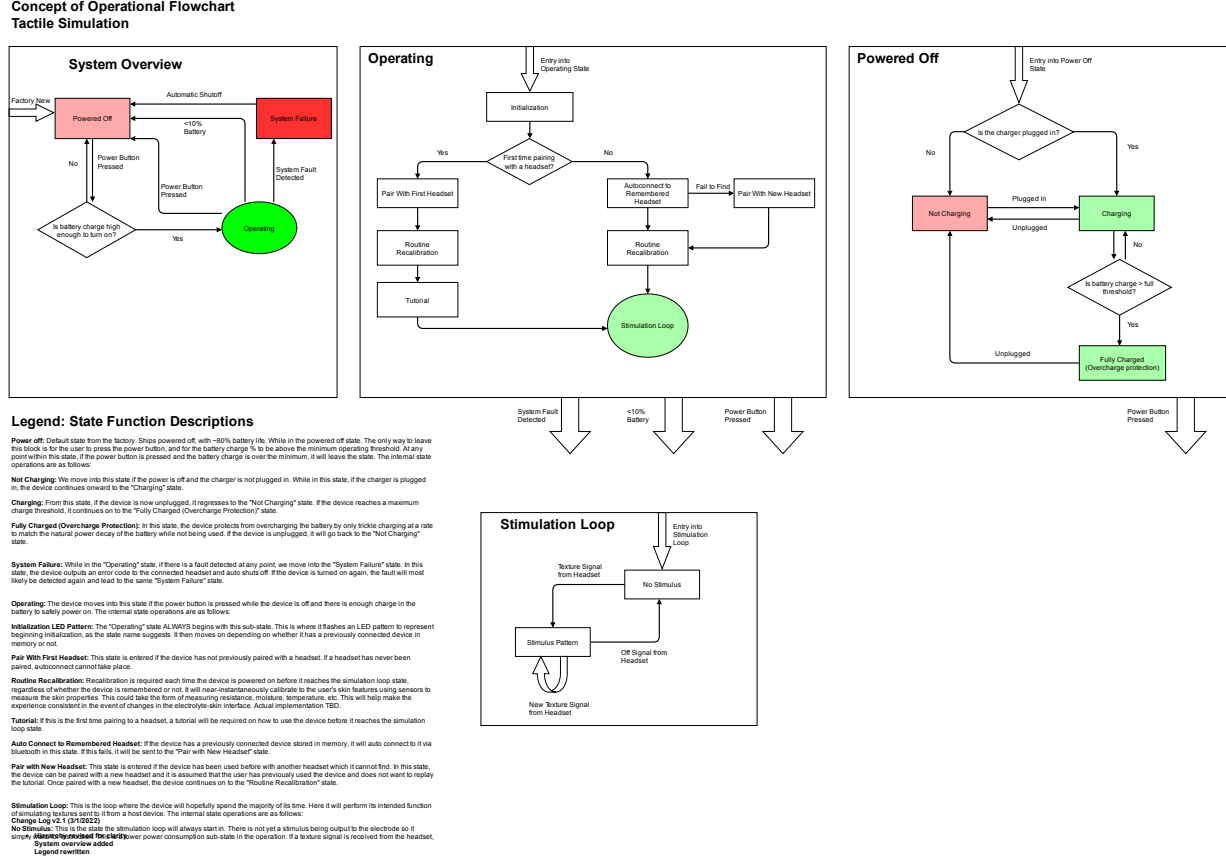


Figure 29: Concept of Operations Flowchart. Outlines the expected use cycle of the final product.

**Success Criteria Matrix**

Criteria	Indicator	Type	Units	Baseline	Result/ Objective	Measurement Strategy
Item/need to be addressed) A successful project will:	(How will you know? What evidence is needed?)	(Qualitative/quantitative)	()	(Current situation)	(Target outcome)	(How will you track the outcome? This must be an actionable item)
Simulated texture feels realistic	Users report realism score	Qualitative	#	0	9/10	Create a VR demo to showcase a variety of textures, run user trials and survey subjects on realism of texture.
	Users cannot distinguish real and simulated textures	Quantitative	% accuracy of users to distinguish real from simulated texture	N/A	60% accuracy	Conduct blind (literally) trials with users, with one finger on the device, one finger on a real texture, and ask them to determine which is real and which is simulated. Theoretical maximum would be 50% accuracy, meaning users will guess which texture is real roughly half the time simply by luck.
Simulated textures improve immersion	Users report increased immersion	Qualitative	#	TBD by control trial	20% higher reported immersion vs control	Conduct trials with a control group in VR without device, experimental group using device. Compare reported levels of immersion. We could potentially work with VR games already in beta tests, integrate the device into the game and collect data, using their other beta testers as a control group. (applicable to other user trials as well).
	Number of simulated textures	Quantitative	#	0	100	Number of textures in library.
	Temporal Resolution	Quantitative	Hz	N/A	500mHz	Finer textures will be simulated temporally, by activating the nerves at a given frequency rather than at different locations on the finger to best mimic the natural nervous response. Different levels of fineness can be simulated by different frequencies of stimulation.

						The temporal resolution is the smallest step in frequency the device can change by.
Spatial Resolution	Quantitative	mm	N/A	1mm		The minimum amount of space between separate simulated objects for the device to distinguish the difference. For example, imagine a word in braille. The standard spacing for braille dots is 2.340mm. The device would need a resolution of 2.340mm for the user to read a word in braille. Applicable to very coarse textures.
Maximum Frequency	Quantitative	Hz	N/A	TBD		The highest frequency signal the device needs to be able to apply to the electrodes. May need to be higher than highest texture to superimpose textures.
Device is ergonomic	User reported comfort score	Qualitative	#	TBD by control trial	8/10	Survey users in other trials on their perceived comfort level during trial
	Time spent by users in game	Quantitative	Hours	TBD by control trial	Greater than or equal to control time	User testing without other features active to isolate the variable of device comfort. Compared to a control with no device being worn. Reduced time in game would be an indicator of discomfort.
	Device fits different hand sizes	Quantitative	r	N/A, current controllers are held, not worn	<0.1	Test discomfort on users with outlier hand sizes and look for correlation between hand size and comfort. By using the time in game experiment described above (treating hand size as the experimental variable) we can measure the discomfort caused by outlier hand size. If there is a high correlation between play time and hand size, that would be a problem, but if there is no correlation ( $r<0.1$ ) then it would indicate that large/small handed

						users do not experience more discomfort. Resource below documents 5th, 50th, and 95th percentile hand sizes in length, breadth and circumference. We will aim to find test subjects at these two extremes. <a href="https://nslis.jsc.nasa.gov/sections/section03.htm">https://nslis.jsc.nasa.gov/sections/section03.htm</a> ex. Min hand length: 15.8cm Max hand length: 18.7cm Min hand breadth: 6.9cm Max hand breadth: 8.6cm
Device has good usability features	Device battery life	Quantitative	Hours	~48	3	Time how long the battery can handle average game sessions without dying.
	Device connectivity range	Quantitative	Meters	5	5	Measuring distance before the performance degrades. 3 meters is the length of the stock headset tether and any further would be superfluous.
	Device weight	Quantitative	grams	175 each hand	500	Measure the weight of the device
	Controller Functionality	Qualitative	Inputs	Controllers Have: Joystick, 4 buttons, Position tracking	Should be able to navigate menus as well as controller	The device should be a usable controller, so that you don't need to use both or switch between them. The devices are being adapted and optimized for (camera) hand tracking, using gestures as buttons. We could use the same gestures as hand tracking.
Device Durability	Comprehensive stress test survival	Qualitative	N/A	TBD by control trial	Satisfactory Performance  Resists: Sitting on, stepping on, dropping from realistic height, hitting a wall during gameplay	We will create multiple tests to simulate repetitive and abusive versions of normal scenarios our device should be able to handle. One example would be dropping the device from a height of 1.8 meters, 10 times. Scoring must be qualitative. We will rate the performance for both how well the device still functions, and if the comfort or usability has been impacted. For example if there are any small connection interruptions minorly affecting functionality. Another example would be if any jagged edges appear during the stress tests affecting the comfort and usability. The objective of the stress tests would be to locate any weak points of the device through exaggerated use to ensure that it holds up to reasonable wear adequately.

	Water/dust proof	Qualitative	Ingress Protection Rating	IP00	IP57	Perform a water and dust ingress test. We are aiming for IP47, meaning protection against access to hazardous parts and protection against dust (5). We should be able to test this to some effect by attacking the device with dust/sand and then seeing how much has made it into the device. It should also be protected against temporary submersion, 30 minutes at 1m depth (7). We could also outsource to a testing company to get a reliable/credible rating.
	Easy to clean	Qualitative	N/A	Controllers are plastic and pretty easy to wipe down	Easy to clean	A cloth glove could get pretty dirty; it may not be realistic to put through the laundry. It should either be launderable if it uses cloth, and have the electrical components either detachable or laundry safe, or it should be a sleek material like plastic that doesn't dirty easily and is easy to wipe off.

#### Change Log v0.1 (11/22/2021)

- First draft completed

#### Change Log v1.0 (12/3/2021)

- Clarification changes made

#### Change Log v1.1 (12/9/2021)

- Changed Changelog v0.1a to v0.1
- Added controller functionality to usability section
- Added easy to clean to durability section
- Added to stress test

#### Change Log v1.2 (12/10/2021)

- Updated Changelog format

Figure 30: Success Criteria Matrix. Defines measurable criteria for quantifying successful implementation of the project.

## References

- [1] Gloria Araiza Illan et al. “A simulation environment for studying transcutaneous electrotactile stimulation.” In: *PLOS ONE* 14.2 (Feb. 2019), pp. 1–30. DOI: 10.1371/journal.pone.0212479. URL: <https://doi.org/10.1371/journal.pone.0212479>.
- [2] Pour Naser Aryan, Hans Kaim, and Albrecht Rothermel. *Stimulation and recording electrodes for neural prostheses*. Springer International Publishing, 2015.
- [3] Texas Instruments Incorporated. “AN-1515 A Comprehensive Study of the Howland Current Pump (Rev. A).” In: (2013). URL: <https://www.ti.com/lit/an/snoa474a/snoa474a.pdf>.
- [4] Texas Instruments. *LM324N-Datasheet*. URL: [https://www.ti.com/lit/ds/symlink/lm324.pdf?ts=1654801853898&ref\\_url=https%5C%253A%5C%252F%5C%252Fwww.ti.com%5C%252Fproduct%5C%252FLM324](https://www.ti.com/lit/ds/symlink/lm324.pdf?ts=1654801853898&ref_url=https%5C%253A%5C%252F%5C%252Fwww.ti.com%5C%252Fproduct%5C%252FLM324).
- [5] K.A. Kaczmarek, M.E. Tyler, and P. Bach-Y-Rita. “Electrotactile haptic display on the fingertips: preliminary results.” In: *Proceedings of 16th Annual International Conference of the IEEE Engineering in Medicine and Biology Society*. Vol. 2. 1994, 940–941 vol.2. DOI: 10.1109/IEMBS.1994.415223.
- [6] Andreas Kuhn. “Modeling transcutaneous electrical stimulation.” PhD thesis. ETH Zurich, 2008.
- [7] Xiong Lu et al. “Experiment Study for Wrist-Wearable Electro-Tactile Display.” In: *Sensors* 21 (2021). ISSN: 1424-8220. DOI: 10.3390/s21041332. URL: <https://www.mdpi.com/1424-8220/21/4/1332>.

- [8] Microchip. *HV507-Datasheet*. URL: <https://ww1.microchip.com/downloads/aemDocuments/documents/OTH/ProductDocuments/DataSheets/20005845A.pdf>.
- [9] Apex Microtechnology. *PA08-Datasheet*. URL: <https://www.apexanalog.com/resources/products/pa08u.pdf>.